

Pulsed fast reactors

V. L. Aksenov¹, A. E. Verkhoglyadov¹, M. M. Podlesnyy*¹, and E. P. Shabalin¹

¹*Joint Institute for Nuclear Research, Dubna, Russia*

Abstract

In 1960, the world's first pulsed fast nuclear reactor (IBR) was created at JINR. The second-generation IBR-2 reactor has been in operation since 1984. An analysis of the distinctive characteristics of the IBR-type reactors is presented, the main one of which is related to the instabilities of power fluctuations. A description of the conceptual design of a third-generation NEPTUN reactor is proposed, which solves the problem of instabilities and opens up new possibilities for neutron beam research.

Keywords: pulsed fast reactors, dynamics of the pulsed fast reactors, neptunium nitride

DOI: [10.54546/NaturalSciRev.200709](https://doi.org/10.54546/NaturalSciRev.200709)

Contents

1. Introduction	1
2. First generation	3
3. Second generation	8
4. Features of the dynamics of pulsed fast reactors	17
4.1. Dynamics of a low-power pulsed fast reactor	17
4.2. Dynamics of a high-power pulsed fast reactor	19
4.3. The influence of dynamic bending on dynamics of a pulsed fast reactor	23
4.4. The influence of static fuel assembly bending on dynamics of a pulsed fast reactor	25
5. Third generation. The NEPTUN reactor	27
5.1. Limitations on neutron flux	27
5.2. The NEPTUN reactor	30
5.3. Why neptunium?	32
6. Conclusion	34

1. Introduction

Within the broad family of pulsed nuclear reactors, a special place is occupied by periodic pulsed reactors, in which bursts of fission are produced by an external modulation of reactivity with a prescribed period. In 1955, D. I. Blokhintsev proposed the concept of such a reactor with periodic reactivity modulation achieved by rotating a part of the reactor core (Figure 1).

*Corresponding author e-mail address: podlesny@phystech.edu

Since fission in this reactor is driven by fast neutrons, it was termed a pulsed fast reactor (Russian abbreviation IBR) [1].

Once during each cycle, with a period ranging from 0.01 to 10 s, the reactor is briefly — for less than one millisecond — transferred from a deeply subcritical state (3–5% in terms of the effective multiplication factor k_{eff}) to a supercritical state with respect to prompt neutrons. This produces a power pulse with a duration of 40–200 μs , while the background power between pulses remains low (4–6% of the average power).

In 1956, at the Institute of Physics and Power Engineering (IPPE, Obninsk), I. I. Bondarenko and Yu. Ya. Stavisskii developed an approximate theory of the pulsed fast reactor; its open publication appeared in 1959 [2]. Reactor design activities were initiated the same year. Also in 1956, the Joint Institute for Nuclear Research (JINR) was founded in Dubna. According to the memoirs of the first Director of JINR, D. I. Blokhintsev [3]: “According to the initial plan, JINR was conceived as consisting of three laboratories, each equivalent to a full institute. Two of them already existed. The third was intended to focus on technological work in nuclear engineering. I proposed establishing a Laboratory of Theoretical Physics, which was immediately supported and approved.

The situation with the Technological Laboratory was more complicated. It would have required creating something like a second Obninsk. . . Then the idea occurred to me — to establish a Laboratory of Neutron Physics instead and to use a periodically operating pulsed reactor, IBR-1, which had just been invented at IPPE in Obninsk, as the neutron source. . . I went to I. V. Kurchatov. . . He approved my proposal and said, ‘Let’s go to the general’ (A. P. Zaveniagin). Thus, with the assistance of Igor Vasilievich, the Laboratory of Neutron Physics was established at JINR. . .”

On June 23, 1960, at the JINR Laboratory of Neutron Physics headed by Nobel laureate Academician I. M. Frank (now the Frank Laboratory of Neutron Physics), the world’s first periodic pulsed reactor started operation [4] (Figure 2). This first-generation reactor underwent a number of upgrades and was finally shut down in 2001. Since 1984, the second-generation reactor IBR-2 (later modernized to IBR-2M) has been operating at JINR. The development of these reactors and the scientific research performed using them were recognized by the USSR State Prize (1971), the Russian Government Prize (1996), and the Russian State Prize (2000).

In the present article, without going into excessive technical detail, we describe the evolution of pulsed fast reactors, highlight the most significant scientific results that influenced the development of science, and discuss future prospects. Particular attention is paid to the project of a third-generation pulsed fast reactor, the NEPTUN reactor, whose parameters and characteristics significantly exceed those of previous generations and are capable of bringing neutron studies of matter to a new level.

This article is an expanded version of our arguments in favor of a fundamentally new reactor design in which the problem of power oscillation instabilities has been resolved, thereby opening new opportunities for physical research. The key points are as follows. First, a characteristic feature of the second-generation IBR reactors is the dynamic instability of power oscillations.

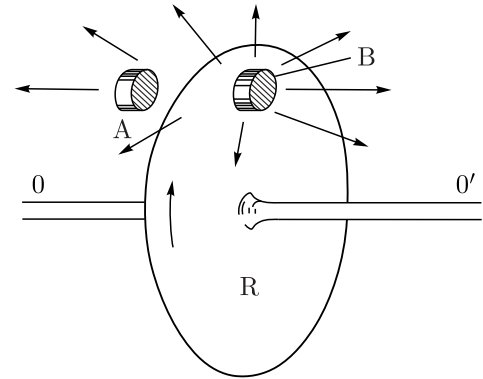


Figure 1. Principle of operation of the periodic pulsed reactor IBR: R — rotor — rapidly rotating disc; B — piece of uranium mounted in the disc; A — stator — stationary piece of uranium; the arrows show the neutron flux at the moment when B passes near A (illustration from D. I. Blokhintsev’s book “The Birth of the Peaceful Atom”).

As fuel burnup increases, this tendency becomes more pronounced, and reactor operation becomes unstable. Eventually, it becomes necessary to substantially reduce the reactor power and, correspondingly, the neutron flux to levels that are marginal or unacceptable for a number of experiments. Second, the parameters of second-generation IBR reactors limit their application primarily to condensed matter physics. An approximately order-of-magnitude increase in neutron flux density achievable with the NEPTUN reactor will make it possible to carry out experiments in nuclear physics as well.

2. First generation

The first generation of pulsed fast reactors includes the IBR reactor (1960–1968), its 1965 modification known as the Superbooster — a hybrid of a pulsed reactor and a microtron accelerator — and the IBR-30 reactor (1969–2001). The latter was a limited-power reactor with a thermal power of 20 kW, featuring fuel elements of reduced diameter and enhanced air cooling. IBR-30 also operated in superbooster mode in combination with the LUE-40 linear electron accelerator.

The design, construction, and commissioning of the first IBR were carried out under the leading role of experienced reactor physicists from Obninsk. In addition to Yu. Ya. Stavisskii, the project involved F. I. Ukraintsev, O. D. Kazachkovskii, N. V. Krasnoyarov, Yu. A. Blyumkina, V. A. Malykh, V. P. Zinoviev, and others. Researchers from the JINR Laboratory of Neutron Physics, led by I. M. Frank (including S. K. Nikolaev, B. N. Deryagin, S. A. Kvasnikov, V. D. Ananiev, E. P. Shabalin, B. N. Bunin, and others), also played a major role. The rotating disk of IBR, with a press-fitted insert of highly enriched uranium manufactured in Obninsk, was developed by a group led by G. E. Blokhin from the Central Institute of Aviation Motors (CIAM). The reactor control and protection system were developed with the participation of CRI-58, while plutonium fuel elements were designed under the leadership of I. S. Golovnin (VNIINM, Moscow). Notably, fuel elements for all subsequent IBR reactors were also developed under his supervision, and their exceptional reliability deserves special mention.



Figure 2. The physical launch group of IBR in the reactor hall, June 1960.

The speed with which the first IBR was created is striking by modern standards: only four years elapsed between the formulation of the concept and the startup of the fully operational facility. The world's first periodic pulsed reactor, IBR, with an average power of 1 kW and a pulse duration of 40 μ s, was commissioned at JINR in Dubna on June 23, 1960 [4]. All subsequent IBR reactors were also built in Dubna, with the exception of the Japanese YAYOI reactor and the series of TRIGA reactors, which can operate only in the regime of rarely repeated pulses (no more frequently than once every few minutes).

In order to simplify the design of this unique, first-of-its-kind reactor, the average power of IBR was deliberately chosen to be low — 1 kW (while the instantaneous power in a pulse reached 5 MW). Later, V. D. Ananiev demonstrated that by increasing the airflow rate for cooling, the average reactor power could be raised to 6 kW. From 1964 onward, the reactor operated at power levels between 2 and 6 kW [5, 6].

Initially, IBR was intended primarily for nuclear-physics applications, such as measurements of total and partial neutron cross sections, neutron resonance parameters, nuclear excitation levels, and related quantities, using neutron time-of-flight spectroscopy. However, soon after startup, a highly successful program devoted to the study of the structure and dynamics of crystalline materials using slow-neutron scattering methods was launched. This direction was initiated by the Polish physicists B. Buras and E. Janik and strongly supported by F. L. Shapiro. The relatively long neutron pulse of the reactor (50 μ s) proved to be particularly well suited to problems in condensed matter physics [7, 8].

The possibility of using the time-of-flight method in neutron diffraction was first discussed by P. Egelstaff in 1954. In 1961, B. Buras attempted to apply this method at a stationary reactor in Świerk (Warsaw) using a Fermi chopper to generate neutron pulses. However, the neutron intensity was insufficient for practical experiments. In 1962, B. Buras and F. L. Shapiro proposed transferring these experiments to the IBR reactor in Dubna. The experiments proved successful and can be regarded as the first practical implementation of neutron diffraction using the time-of-flight method (Figure 3). Subsequently, at the IBR-30 reactor, researchers of the Laboratory of Neutron Physics developed essentially all major methodologies in this field that were later adopted at other pulsed neutron sources worldwide.

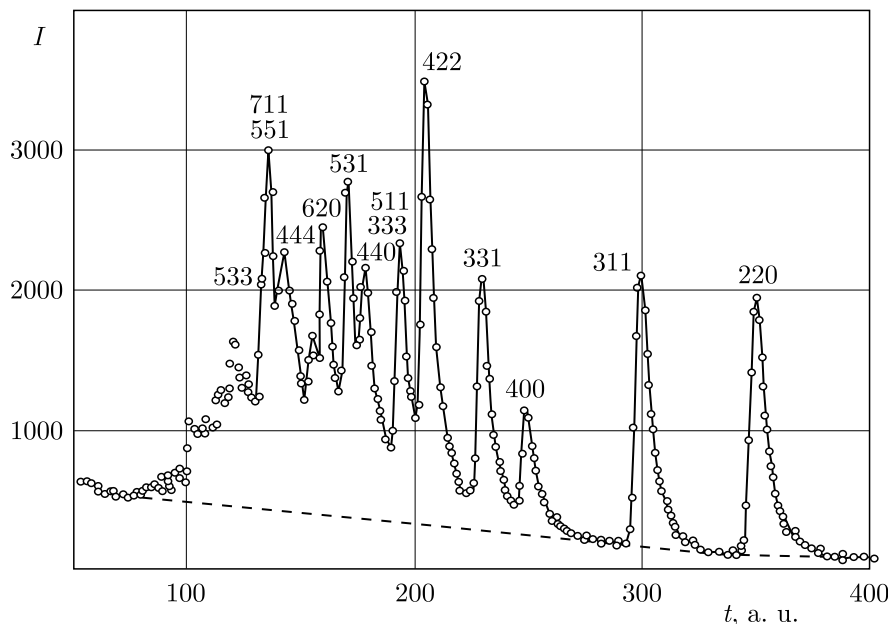


Figure 3. Neutron diffraction pattern of Si, measured at IBR-1. $\Delta d/d \approx 0.02$ [7].

With the emergence of high-flux pulsed neutron sources in the mid-1980s, the time-of-flight method in neutron diffraction evolved into a powerful tool for structural research and became widely used. Several factors contributed to this development. These include the great flexibility in experimental design, particularly the possibility of simultaneous scanning in both wavelength and scattering angle; the ability to record diffraction patterns at a fixed scattering angle, which significantly expanded the range of external pressures applicable to samples; and the capability to obtain three-dimensional (3D) neutron diffraction patterns using a two-dimensional position-sensitive detector with time of flight serving as the third coordinate. This proved exceptionally useful for studying incommensurate structures and incoherent diffuse scattering arising during structural phase transitions.

To shorten the neutron pulse, the first IBR reactor, following a proposal by F. L. Shapiro, began operating in 1964 in a neutron pulse multiplication mode using a neutron-producing target driven by an electron microtron (Figure 4). A leading role in the development of the microtron was played by I. M. Matorin, S. P. Kapitsa (Institute for Physical Problems, USSR Academy of Sciences), and R. V. Kharyuzov [9]. With the commissioning of the pulsed booster (this was the name given to the accelerator–IBR tandem), the neutron pulse duration was reduced to $3 \mu\text{s}$, and the pulse quality factor of the neutron source N/θ^2 , introduced by F. L. Shapiro (where N is the neutron intensity or flux at the moderator surface and θ is the neutron burst duration),

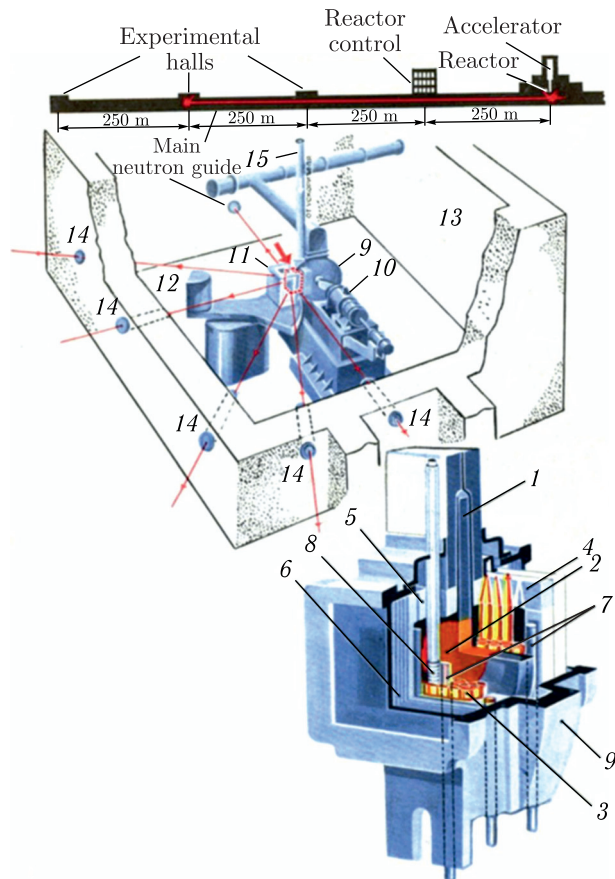


Figure 4. Pulsed fast reactor IBR: 1 – rotating steel disk; 2 – movable fissile part (uranium); 3 – fuel rods in the stationary part; 4, 5 – support structures; 6 – neutron reflector; 7 – control elements; 8 – neutron-production target of electron accelerator; 9 – reactor vessel; 10 – disk drive motor; 11 – neutron moderator; 12, 13 – biological shielding; 14 – neutron guides; 15 – electron beam guide.

increased by nearly two orders of magnitude. Subsequently, the microtron was replaced by a more intense linear resonance accelerator [10].

In 1966, the IBR reactor implemented an operating mode with variable pulse amplitude, as well as a mode of rare pulses with a repetition period of 5 s. Realization of this mode required a reactivity modulator consisting of three synchronized movable elements. Two fast modulators were identical to those used in the standard 5–10 Hz mode, namely rotating steel disks with uranium inserts. The third element was an oscillating tungsten rod moving vertically. In the rare-pulse mode, the peak power reached 1 GW.

The IBR-1 reactor was shut down in August 1968. Notably, the final experiment performed at this reactor was the first observation of ultracold neutrons (UCN) (Figure 5), carried out precisely in the rare-pulse mode [11].

In the first observation of UCN, their density was only about 10^{-5} UCN per cubic centimeter. Over time, UCN research involved numerous scientific centers in the USSR and abroad, including Moscow (five institutes), Dubna, Gatchina, Alma-Ata, Melekes, and Lytkarino, as well as laboratories in Germany, Canada, the United Kingdom, France, and the United States. A wide range of research reactors was employed for UCN production, from low-power university reactors (0.5 MW) to the high-flux SM-2 reactor (100 MW) with record neutron fluxes [12]. In total, more than forty different types of neutron guide systems and related extraction devices for UCN were constructed worldwide. Experimental groups investigated UCN generation, transport, spectroscopy, storage, and detection. At present, the maximum achievable UCN density is ~ 100 UCN per cubic centimeter, i.e., seven orders of magnitude higher than in the first experiment. The storage time of UCN in material traps is now primarily limited by the beta decay of free neutrons (~ 900 s). All these results were obtained almost entirely empirically; theoretical descriptions of UCN phenomena have so far achieved only limited success. At present, the most significant achievements of UCN-based fundamental experiments include a substantial reduction of the upper limit on the neutron electric dipole moment $d_n < 0.18 \cdot 10^{-25}$ e·cm

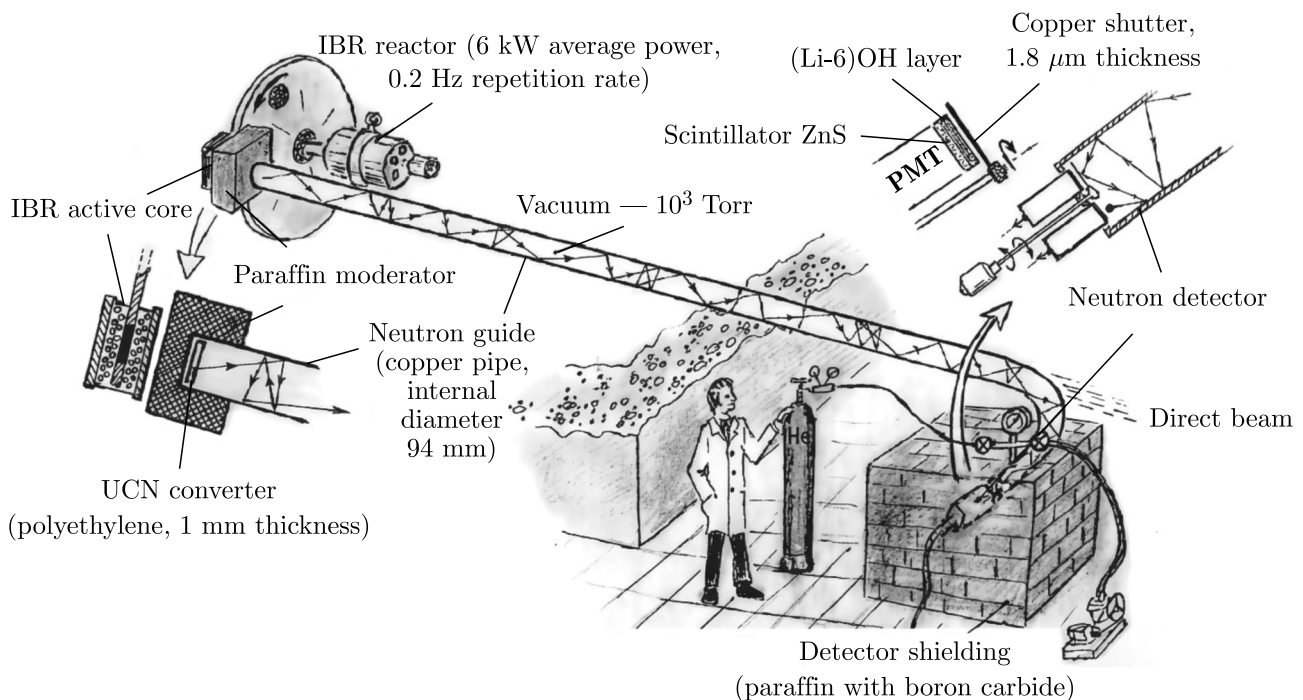


Figure 5. Schematic of the experiment on the observation of UCN at FLNP JINR.

and high-precision measurements of the free neutron lifetime $\tau_n = (878 \pm 0.5) \text{ s}$, which are key constants for understanding the fundamental laws governing the microworld [13].

On June 10, 1969, an improved successor of the IBR reactor, IBR-30, was commissioned. The designation “30” refers to the design average power of 30 kW, although in practice the reactor operated at 20–25 kW. The power increase was achieved by modifying the plutonium fuel element design and introducing two uranium inserts (reactivity modulators) into the rotating steel disk instead of one. The rare-pulse mode, with pulse repetition periods of up to 13 s, was retained. Mechanical failures in the drive system of the tungsten rod led to an accident at IBR-30 in 1972. Following this event, the mode of rare periodic pulses was permanently abandoned.

The booster mode (IBR-30 operated alternately as a reactor and as a booster until 1986, when reactor-mode operation was terminated) was implemented using the LUE-40 linear resonance accelerator as an injector, providing electron energies of 44 MeV and a pulse current of 0.2 A. In the booster mode, the average power was 10 kW, with a half-width of the fast-neutron burst of approximately $4 \mu\text{s}$.

The high brilliance of the spectrometers at IBR-30 enabled the discovery of several entirely new research directions in nuclear physics and condensed matter physics [14]. Particularly well known are studies of hyperfine neutron–nucleus interactions, parity nonconservation effects, rare (n, α) reactions in neutron resonances, and related phenomena. In 1971, the work on the development of IBR-type reactors and pulsed booster systems was awarded the USSR State Prize.

Among the scientific directions that had a profound impact on the development of nuclear and neutron physics were studies of polarized nuclei using polarized neutrons. The idea of producing polarized neutrons by transmission through a polarized proton target at a high-brightness pulsed IBR reactor was proposed in 1963 by the Scientific Leader of the laboratory, F. L. Shapiro. As early as the following year, this concept was successfully implemented under his guidance by P. Dragicescu, V. I. Lushchikov, V. G. Nikolenko, and Yu. V. Taran. Subsequently, the same group, in collaboration with V. P. Alfimenkov, solved the problem of creating polarized targets of holmium and deuterium nuclei (the POLYANA facility, Figure 6). Using

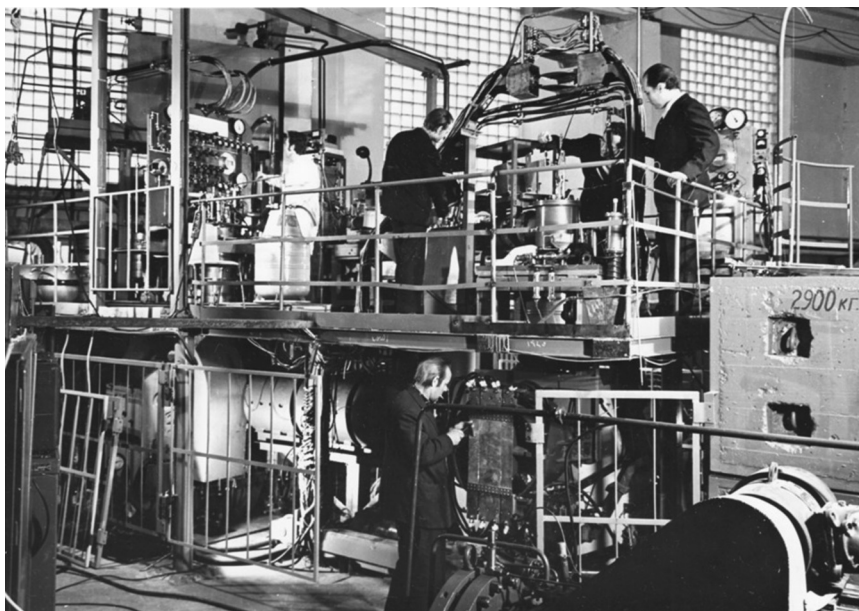


Figure 6. External view of the POLYANA experimental setup.

this setup, experiments were performed to determine the spins of compound nuclear states of ^{165}Ho , and the neutron–deuteron scattering lengths were unambiguously determined for the first time [15].

In the early 1980s, under the leadership of L. B. Pikelner, with the participation of V. P. Alfimenkov, S. B. Borzakov, Vo Van Tuan, Yu. D. Mareev, A. S. Khrykin, and E. I. Sharapov, pioneering studies of P-parity nonconservation effects in p -wave neutron resonances of ^{139}La and ^{117}Sn were carried out using beams of polarized resonance neutrons. These experiments confirmed the large enhancement of P-odd effects predicted by theory, compared with those previously observed using thermal neutrons [13].

These experiments initiated an extensive international research program on P-odd dichroism effects, including work at Los Alamos, as well as measurements of P-violating effects in the (n, y) and (n, f) reactions in Dubna and Gatchina.

Later, in the 1990s, in collaboration with colleagues from PNPI (Gatchina) and IPPE (Obninsk), a series of experiments was performed at the IBR-30 + LUE-40 source to measure P-even and P-odd angular correlations of fission fragments from U-235 and Pu-239 nuclei. These experiments employed polarized neutrons and aligned nuclear targets. The resulting data were successfully analyzed using an original theoretical approach developed at the Frank Laboratory of Neutron Physics in collaboration with the Kurchatov Institute.

These methodologically very complex experiments remain unique to this day and have not been reproduced elsewhere.

The IBR-30 booster was shut down in 2001, with the intention of replacing it by a booster with a substantially shorter neutron pulse, better suited for research in fundamental and applied nuclear physics. Development of the new booster project was led and actively promoted by V. L. Aksenov, Yu. P. Popov, and V. T. Rudenko. An open competition was announced for the construction of a new linear accelerator for the booster, with demanding initial specifications: a beam power of 10 kW, a pulse duration not exceeding 250 ns, a repetition rate of 100–150 Hz, and a total accelerator length not exceeding 8 m. The competition was won by the team of the Budker Institute of Nuclear Physics, Siberian Branch of the Russian Academy of Sciences.

In 1992, with the active participation of V. L. Lomidze, A. K. Krasnykh, and V. I. Furman, the concept of a new neutron source, termed a Source of Resonance Neutrons (Russian abbreviation IREN), was finalized [16]. The IREN project was officially granted the status of a new JINR basic facility at the 75th session of the JINR Scientific Council in May 1994. At the same time, V. I. Furman was appointed Project Leader, V. D. Ananiev became Chief Engineer, and A. K. Krasnykh was assigned responsibility for the accelerator component of IREN. NIKIET served as the developer of the target system design, and plutonium fuel elements were manufactured at the Mayak Production Association. Unfortunately, the neutron multiplication target mode was not implemented.

3. Second generation

As a result of the successful launch of the program devoted to studies of the structure and dynamics of condensed matter at the first IBR reactor, preliminary feasibility calculations aimed at justifying the creation of a significantly more powerful fast pulsed reactor were initiated as early as 1963 [17]. The goal was to develop a neutron source whose characteristics for slow-neutron scattering experiments would be comparable to those of 50–100 MW stationary research reactors — such as the HFR at the Institut Laue–Langevin (Grenoble), SM-2 at NIIAR (Dimitrovgrad), and PIK at PNPI (Gatchina) — as well as to proton-accelerator-based sources that at that time existed only at the conceptual level (spallation neutron sources, SNS).

Intensive work on the development of a pulsed reactor with an average power of 5–10 MW, designated IRM, began in 1967, following the publication of projects for powerful IBR-type reactors in Europe (SORA) [18, 19] and in the United States (Brookhaven National Laboratory) [20].

None of these foreign projects, however, was ultimately realized. It should be noted that these designs contained fundamental, critical deficiencies that would have prevented them from achieving their declared parameters in terms of power and pulse duration. For example, the Brookhaven reactor design, nominally rated for an average power of 30 MW, would in practice have been able to operate only at a few megawatts due to the so-called pulse instability, which is intrinsically inherent to periodic pulsed reactors and was first identified at FLNP [21, 22].

In contrast, at Dubna a new reactor with a design power of 4 MW, termed IBR-2, was constructed by 1977 with the participation of NIKIET, GSPI, VNIINM, and other institutes and organizations of the USSR and JINR Member States. The physical startup was completed in 1978, while official routine operation began in April 1984 [23, 24]. The prolonged commissioning period was explained by the novelty of the problem and the desire to minimize the risk of pre-accident situations. For reasons of nuclear safety and operational reliability, the average reactor power was limited to 2 MW, and the pulse duration turned out to be 216 μs instead of the design value of 90 μs . Nevertheless, even with these parameters, IBR-2 became and remains one of the most effective pulsed sources of slow neutrons for condensed matter research.

The design of the IBR-2 core was primarily dictated by the requirement to achieve very high neutron fluxes, on the order of $10^{16} \text{ cm}^{-2} \cdot \text{s}^{-1}$ in a pulse, combined with short pulse durations. This is possible only in a reactor with a power of several megawatts. As a result, it was necessary to abandon the fundamental layout used in first-generation IBR reactors, since it could not provide adequate heat removal from the moving reactivity-modulator elements containing fissile material. For IBR-2, a different scheme was adopted [25, 26], in which reactivity modulation is achieved by moving neutron reflectors in the vicinity of the core (Figure 7).

Because the reflector material contains no fissile components, heat removal is readily provided by a flow of gaseous helium. The movable reflector acting as the reactivity modulator consists of two blades of complex shape, each with a diameter of 2.4 m and a mass of several hundred kilograms. The blade of the main reflector rotates at speeds of up to 1500 rpm in a plane parallel to the tangent to the core surface. A power pulse is generated when both blades simultaneously pass close to the core. To ensure nuclear safety and pulse-to-pulse stability, the blade-rotation mechanism is manufactured with exceptionally high precision. Fluctuations of the blade tip position during passage near the core do not exceed several tens of micrometers. A dedicated electronic system continuously monitors reflector stability.

The requirement to obtain high neutron fluxes at short pulse durations also necessitated the creation of a compact core with high specific power density and a short neutron lifetime. A plutonium-oxide core with sodium cooling was selected, analogous to the core of the BR-5 reactor constructed at IPPE in the 1960s. This solution made it possible, on the one hand, to

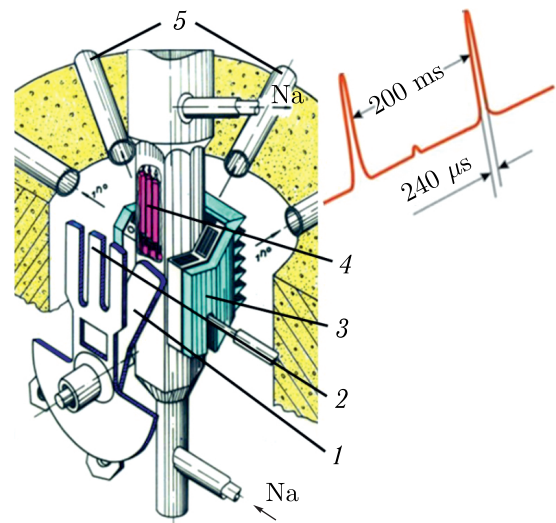


Figure 7. Scheme of neutron pulse generation: 1 — main movable reflector; 2 — auxiliary movable reflector; 3 — water moderator; 4 — core; 5 — neutron guides.

satisfy the neutron-source requirements and, on the other, to rely on proven technical solutions and a well-developed industrial technology for the fabrication of the core and for the operation of the sodium cooling system. The sodium cooling system has operated successfully and continuously since its commissioning in 1981, both during reactor operation and during shutdown periods.

The movable reflector is one of the most critical and technically original components of IBR-2 (Figure 8). It has no analogs not only in reactor engineering but also in other fields of



Figure 8. Movable reflector of the IBR-2 reactor.

technology. It is precisely this component that determines the pulse duration of the reactor — its most important parameter — on which the resolution of neutron spectrometers depends in both diffraction and inelastic-scattering experiments. The probe particle used to study the structure and dynamics of matter is the thermal neutron, whose diffusion time in hydrogen-containing materials of the external moderator is 100–200 μs . Consequently, the desired duration of the fast-neutron pulse is of the order of 100 μs . The first version of the movable reflector used during the physical startup of IBR-2 in 1978 could not provide pulses shorter than 300 μs in routine operation. This was due to the fact that the auxiliary movable reflector is optimally placed behind the main reflector, which is closer to the core, in order to increase the solid angle available to experimental instruments. However, this configuration gives rise to a reactivity shadowing effect, caused by mutual screening of the reflector blocks. This effect reduces the rate of reactivity change during pulse formation and leads to an increase in pulse duration. As a result of extensive com-

putational and experimental studies conducted at FLNP on the EPOS test facilities [27, 28], a configuration of the auxiliary reflector — known as the “trident” geometry — was identified in which the shadowing effect is negligible. Three such reactivity modulators with trident-type auxiliary reflectors were used at IBR-2 from startup until 2003, each for periods of 6–7 years.

The detrimental shadowing effect of reactivity can be transformed into a beneficial one when both movable reflectors have a toothed (or grid-type) structure. The concept of such a reactivity modulator was proposed by FLNP staff as early as 1971 [29]. The idea is that, for a grid-type geometry, the main and auxiliary movable reflectors rotate in opposite directions. In this configuration, the reactivity changes by a significant amount over a very short time interval equal to the mutual overlap time of the “teeth,” thereby ensuring a short power-pulse duration. For the IBR-2 reactor, a modulator of this type was developed for operation at high rotational speeds of the main and auxiliary reflectors (1500 and 1200 rpm, respectively), which would have provided a power-pulse half-width of $(110 \pm 5) \mu\text{s}$, compared with 216 μs for the trident-type auxiliary reflector at the same rotational speed. However, financial constraints in the 1990s prevented the implementation of this design, since such a complex and expensive machine would have had to be manufactured approximately every five years. Instead, a grid-type reflector made of a nickel alloy was developed for operation at reduced rotational speeds while maintaining the pulse duration. It was successfully commissioned at the reactor in 2004, demonstrating a pulse width of approximately 220 μs at a main-reflector speed of only 600 rpm. Operation at lower rotational speeds significantly extends the safe service life of the movable

sources (SNS). However, the low pulse repetition frequency of IBR-2 combined with the high peak neutron flux density at the moderator surface ($5 \cdot 10^{15} \text{ cm}^{-2} \cdot \text{s}^{-1}$ for wide beams and up to $10^{16} \text{ cm}^{-2} \cdot \text{s}^{-1}$ for collimated beams) are regarded as an advantage of reactor-based neutron sources. This makes it possible to explore a wide momentum-transfer range, study weakly scattering samples, and use tight collimation to improve spatial resolution. The relatively long pulse duration (approximately $320 \mu\text{s}$ for thermal neutrons) was previously considered a natural drawback of IBR-2 because it limited the time resolution of spectrometers employing traditional techniques.

The introduction of Fourier diffractometry and other modern methods fundamentally changed this situation [7]. Owing to its record-high peak thermal-neutron flux, IBR-2 offered significant advantages in diffraction experiments not requiring high resolution. However, precision measurements with accuracy at the 1% level were initially unattainable.

For IBR-2, the conventional approach of increasing the flight path length is not applicable because the thermal-neutron pulse width is $\Delta t_0 = 320 \mu\text{s}$. Therefore, the reverse time-of-flight method using a Fourier chopper was proposed and adapted for use at IBR-2.

The implementation of the Fourier diffractometer at IBR-2 was of fundamental importance. First, it enabled precision structural investigations that were immediately applied to the study of new materials. Second, it demonstrated that, when used skillfully, long-pulse neutron sources can provide capabilities essentially comparable to those of short-pulse accelerator-based sources, while the latter are one to two orders of magnitude more expensive. This experience has since been adopted worldwide. Figure 10 shows a diffraction pattern of a silicon test sample measured with the Fourier diffractometer, compared with the first time-of-flight measurements shown in Figure 3.

Progress in many areas of science and technology is directly associated either with the discovery of unusual properties in already known materials or with the emergence of new chemical compounds. A well-known example, including to non-specialists, is the discovery in the late 1980s of an entire family of compounds in which the superconducting state (i.e., the absence of electrical resistance) appears at relatively high temperatures.

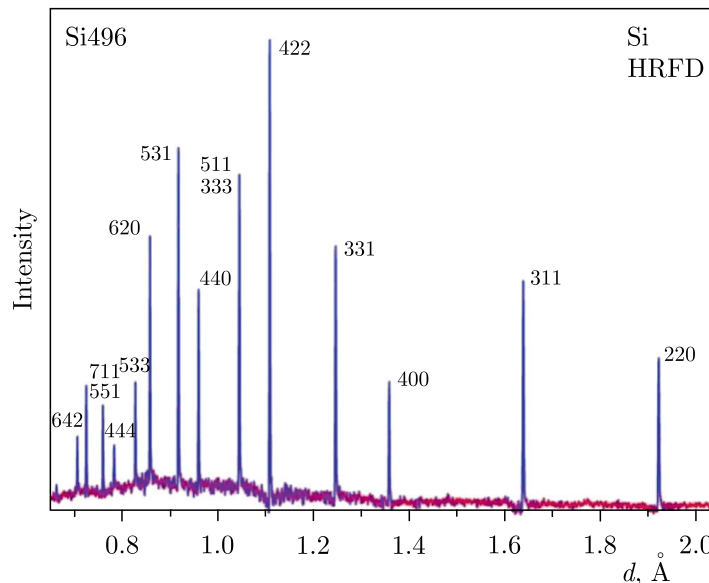


Figure 10. Neutron diffraction pattern of Si measured at IBR-2 using Fourier diffractometry (1996), $\Delta d/d \approx 0.0011$ [8].

One of the most illustrative examples of the effectiveness of neutron methods in structural studies is the determination of the crystal structure of high-temperature superconductors (HTSCs). Their discovery in 1986 became one of the most significant events in physics, long anticipated and provoking a tremendous response not only in the scientific community but also in the broader public sphere. It is sufficient to note that already in 1987 the Nobel Prize in Physics was awarded to the Swiss scientists K. A. Müller and J. G. Bednorz for this discovery.

The presence of very heavy elements in mercury-based HTSCs made structural investigations using X -ray diffraction extremely difficult. The central questions concerned the role of oxygen in the formation of superconducting properties, yet oxygen is practically invisible against the background of mercury and barium in X -ray studies. In contrast, neutron–nucleus interactions exhibit no systematic dependence on atomic number; therefore, the light oxygen atom is as visible to neutrons as barium or mercury. A series of experiments conducted in Dubna on mercury-based HTSCs, including diffraction measurements at different temperatures and pressures and on samples with varying oxygen content, made it possible to answer several fundamental questions simultaneously. First of all, the oxygen concentration corresponding to the maximum superconducting transition temperature was determined.

The JINR experiments investigating the relationship between the superconducting transition temperature and structural features of Hg-based HTSCs confirmed the special role of antiferromagnetic exchange interaction between copper and oxygen in the geometrical plane of the CuO_2 compound for spins $S = 1/2$ located at copper lattice sites. It was also demonstrated that, in Hg-based HTSCs, the Cu–O–Cu bond angle in the copper–oxygen plane is close to 180° , which ensures the maximum value of the antiferromagnetic exchange interaction.

It is indicative that some of the target designs for projected spallation neutron sources are oriented toward long neutron pulses with durations on the order of milliseconds. The current neutron-scattering capabilities of the best existing SNS–ISIS in the United Kingdom (Rutherford Appleton Laboratory), commissioned later than IBR-2 — do not exceed those of IBR-2. Only recently has a powerful SNS entered operation in the United States (Oak Ridge), whose parameters significantly surpass the current performance of IBR-2.

Traditional neutron sources — steady-state research reactors — continue to be used for experiments employing slow neutrons. Reactors with high neutron fluxes are generally multipurpose facilities and offer greater versatility. However, the construction and operation of such reactors are an order of magnitude more expensive than those of IBR-2. Moreover, for a wide class of experiments utilizing the neutron time-of-flight method, IBR-2 has clear advantages over steady-state reactors. The accelerator-based sources mentioned above are even more costly.

The development of the IBR-2 pulsed research reactor was awarded the Government Prize of the Russian Federation in 1997, and the scientific work on the implementation of time-of-flight neutron diffraction methods at pulsed sources at the Frank Laboratory of Neutron Physics received the State Prize of the Russian Federation in 2000.

Any reactor has a finite service life due to the development of radiation-induced “fatigue” in structural materials. In the mid-1990s, the Chief Engineer V. D. Ananiev and the Director of FLNP V. L. Aksenov initiated a modernization program for IBR-2 aimed at replacing the majority of its components whose service life was expected to expire by 2007. In addition to replacement, the modernization involved substantial improvement of key systems — such as the reactor vessel, stationary reflector, emergency protection actuators, and external neutron moderators — in order to increase reliability and operational lifetime. Furthermore, a new

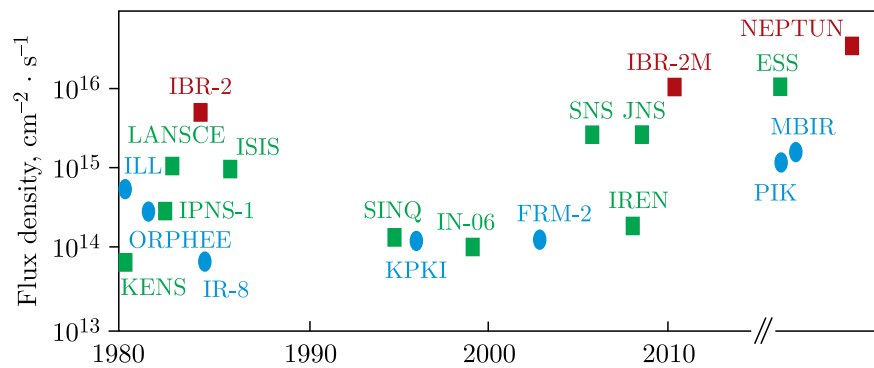


Figure 11. Evolution of high-flux neutron sources. Steady-state reactors (●) and accelerator-based sources (■) have reached their technological limits in thermal neutron production, whereas pulsed reactors (■) retain significant development potential (Y axis is peak flux for pulsed neutron sources).

concept for the configuration and placement of neutron moderators around the modernized reactor, designated IBR-2M, was developed, providing optimal conditions for efficient use of upgraded and newly created spectrometers.

A key issue in preparing for modernization was fuel supply for IBR-2M. This process is described in detail in the memoirs of the principal contributor, A. I. Babaev [32]. The modernization began in 2006 and was completed in 2011. In 2012, the IBR-2M reactor was recommissioned and, as shown in Figure 11, reclaimed its position among the world’s leading neutron sources for experiments on extracted beams.

On IBR-2M, many experimental techniques and research programs have continued to develop. A new, globally unique scientific direction — resonant polarized neutron reflectometry — was established. In 1998–2001, V. L. Aksenov and Yu. V. Nikitenko [33, 34] proposed a method for registering changes in the neutron spin state within a resonantly enhanced neutron wave field under conditions of total reflection of polarized neutrons from multilayer quasi-two-dimensional nanostructures and superconductor/ferromagnet heterostructures. New effects of superconductivity on magnetic states were discovered, with potential applications in modern micro- and nanoelectronics. IBR-2M now hosts the only experimental facility worldwide dedicated to this novel direction in neutron reflectometry [35].

It should be noted that reflectometric studies have been carried out at FLNP since the 1980s, when, at the IBR-2 reactor, the world’s first polarized-neutron spectrometer at a pulsed neutron source was created under the leadership of D. A. Korneev and the Polish physicist A. Bajorek [36]. In 1994, a dedicated polarized-neutron reflectometer, REFLEX, was commissioned [37]. In the early 2000s, this instrument was used to experimentally confirm, for the first time, the effects of Zeeman splitting in neutron reflection from magnetically noncollinear media, as predicted by V. K. Ignatovich. In 2004, with support from the JINR–BMBF (Germany) cooperation program, the polarized-neutron grazing-incidence scattering spectrometer REMUR was constructed [38]. In 2013, within the framework of the user-oriented policy development in the JINR Member States, the neutron reflectometer GRAINS [39] was commissioned for studies of interfaces involving liquid media. This facility was created in collaboration with the Kurchatov Institute — PNPI and with support from the JINR–BMBF (Germany) cooperation program.

In the very first year of operation of the modernized IBR-2M reactor, a cold neutron moderator was installed (Figures 12, 14), developed at the Frank Laboratory of Neutron Physics, JINR [40, 41]. The commissioning took place on July 10, 2012. On three of the fourteen ex-

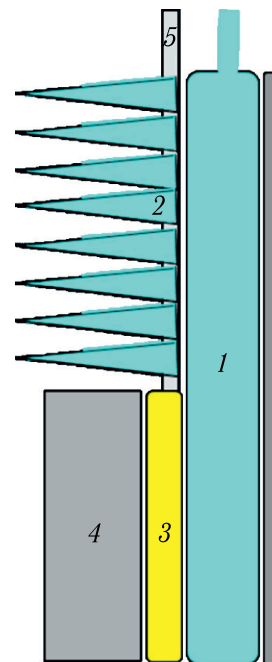


Figure 12. Sketch of the cold combined moderator at the IBR-2M reactor: 1 – water pre-moderator; 2 – comb moderator; 3 – cold chamber with mesitylene pellets; 4 – beryllium filter; 5 – helium and pellets supply pipe.

tracted neutron beams, the flux of cold neutrons with wavelengths longer than 0.4 nm increased by a factor of 13–14, reaching $6 \cdot 10^{11} \text{ cm}^{-2} \cdot \text{s}^{-1}$, i.e., a level comparable to that of the then still design-stage solid-methane moderator of the second target station at the ISIS source.

The design principle of the cold moderator is based on the use of pellets made of a frozen mixture of aromatic hydrocarbons – mesitylene and *m*-xylene (Figure 13). This solution ensures long-term operation of the moderator, up to 10 days, in a fast-neutron flux of up to $2 \cdot 10^{13} \text{ cm}^{-2} \cdot \text{s}^{-1}$ without intermediate warm-ups. The solid-methane moderator previously used at the IBR-2 reactor required warm-up every 8 h, which reduced its operational efficiency by several times. That moderator also had a relatively short service life (Table 1).

The cold moderator chamber (3), located downstream of the water pre-moderator (1), is supplied from above with a cold-helium feed pipe and a pellet delivery tube (5). The bottom of the chamber is made as a mesh with cell dimensions smaller than the pellet size (3.5–4 mm). From below, a cold-helium exhaust pipe and a drain pipe for removing the liquid spent mesitylene are connected to the chamber.

Solid pellets made from a mixture of mesitylene with pseudocumene or *m*-xylene are periodically (once per reactor cycle) replaced in the moderator chamber by melting and draining

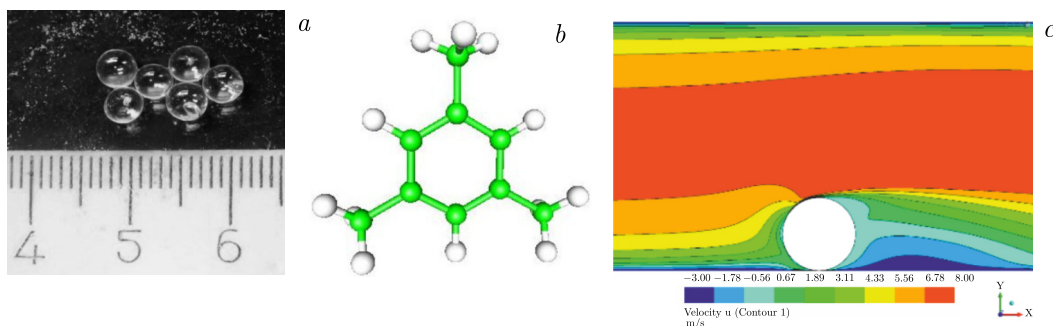


Figure 13. a) Pellets of a frozen mixture of mesitylene and *m*-xylene. b) A mesitylene molecule. c) A pellet in a gas flow: averaged speed of gas is 8 m/s; the speed of the ball is 3 m/s.

Table 1. Pulsed cold neutron sources.

Material	Name and location	Condition	Cold neutron flux $10^{12} \text{ cm}^{-2} \cdot \text{s}^{-1}$	Number of bundles
Liquid H ₂	ISIS, RAL	In operation since 1985	1	5
Solid CH ₄	ISIS, RAL	Replaced regularly	0.6	7
Solid CH ₄	IPNS, ANL	1994–?	0.25	—
Solid CH ₄	CM, IBR-2, JINR	1999–2000	1.2	4
Liquid H ₂	STS, ORNL	Since 2025	~ 3.5	—
Solid C ₉ H ₁₂	CM-1, CM-2, IBR-2M, JINR	Since 2012	0.6	7

the irradiated substance in liquid form. In the frozen state, this mixture has an amorphous structure, which is important in several respects — both for increasing the yield of cold neutrons and for producing uniform, mechanically stable pellets.

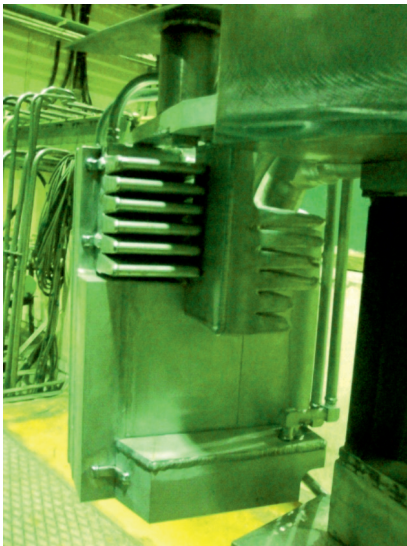


Figure 14. Combined moderator at the IBR-2M reactor with two comb moderators.

At the beginning of an operating cycle, the cooled chamber is filled with pellets delivered from a dispenser by a flow of cold helium at a temperature of 50–60 K. During normal operation, the pellets are additionally cooled by gaseous helium with an inlet temperature below 20 K. At the end of the operating cycle, the duration of which is limited by the maximum permissible viscosity of the irradiated substance in the liquid phase (the viscosity rapidly increases due to the formation of heavy hydrocarbons), the helium flow is stopped and the mesitylene is drained in liquid form into a vessel for subsequent disposal. The chamber and the entire cooling circuit are then purged of residual mesitylene with a flow of warm helium, after which the operating cycle is repeated.

The method for producing solid mesitylene pellets is based on freezing droplets of liquid mesitylene in nitrogen. A crucial factor for obtaining homogeneous solid pellets proved to be the addition of a certain amount of *m*-xylene to the liquid solution. This results in an amorphous structure that is more resistant to cracking. One of the most labor-intensive tasks was mastering the technique of delivering the pellets to the chamber along a long curved transport line with a length of 25 m. It was necessary to completely eliminate pellet blockage and to load ~ 20 000 pellets into the chamber within a short time of no more than one hour.

Later, in 2024, a second cold “combined moderator” was commissioned at the IBR-2M reactor. In both moderators, the concept of combining a cold moderator and water comb-type moderators within a single unit was implemented. Such an original layout provides optimal conditions for neutron utilization along three different beam directions or for obtaining a broad energy spectrum in a selected direction.

4. Features of the dynamics of pulsed fast reactors

4.1. Dynamics of a low-power pulsed fast reactor

The theory of kinetic processes in pulsed reactors was first developed at the Institute of Physics and Power Engineering (Obninsk) by Igor Ilyich Bondarenko and Yuri Yakovlevich Stavisskii (it was termed the B&S theory). The first pulsed (or periodically operated pulsed) reactor, IBR, designed there, was intended to operate at a low power of 1 kW with a pulse repetition frequency from 5 to 50 Hz (a power of 1 kW corresponds to a plutonium fission rate of approximately $3.1 \cdot 10^{13}$ fissions per second). With a critical mass of about 20 kg, the heating of the nuclear fuel during a single pulse did not exceed 0.1 K. Therefore, the authors of the theory quite deliberately and reasonably neglected the influence of temperature on dynamic transient processes in IBR, as well as Doppler effects in neutron resonances. This theory was subsequently referred to as the kinetic theory of a pulsed reactor, since it does not take into account the influence of dynamic factors (deformations, displacements of nuclear fuel) on the neutron multiplication factor in the reactor. Nevertheless, the B&S theory accurately described the dynamics of first-generation IBR reactors and proved to be sufficiently effective during the operation of the IBR-2 and IBR-2M reactors at moderate fuel burnup.

In the B&S theory, the time dependence of the neutron density is described using a point-kinetics reactor model, which is represented by a system of nine first-order differential equations:

$$\begin{cases} \dot{n}(t) = \frac{1}{\tau} (n(t) \varepsilon(t) + S(t) / \nu), \\ S(t) = \sum_{j=1}^8 c_j(t) \lambda_j, \\ \dot{c}_j(t) = n(t) \beta_j - \lambda_j c_j(t). \end{cases} \quad (1)$$

Here, $n(t)$ is the instantaneous neutron fission rate in the reactor; $\varepsilon(t)$ is the time dependence of reactivity (the deviation of the neutron multiplication factor from unity) due to rotation of the uranium-insert disk in first-generation reactors, the movable reflector in IBR-2, or the titanium hydride disk in the NEPTUN reactor; τ is the mean neutron generation time; ν is the number of neutrons per fission; c_j is the concentration of delayed-neutron precursors of group j ; β and λ are the fraction and decay constant of the j -th delayed-neutron group, respectively.

Within the B&S approximation, the solution of system (1) for a pulsed reactor, where $\varepsilon(t)$ is a periodic function of time, can be divided into two stages: a short time interval corresponding to pulse generation $2t_1$ (Figure 15), and the decay of delayed-neutron precursors in the interval

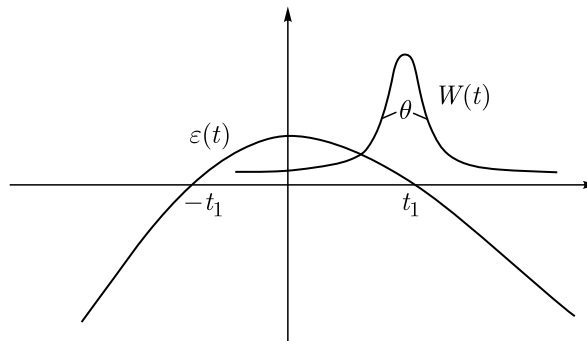


Figure 15. Graph of the change in reactivity $\varepsilon(t)$ and power $W(t)$.

between pulses. The short neutron generation time τ in a pulsed IBR-type reactor (of the order of 10–100 ns), and correspondingly the short duration of the fission pulse (less than one millisecond), with a pulse repetition period shorter than the lifetime of the shortest-lived delayed-neutron group, makes it possible to solve the system separately: only the first equation during the pulse-generation interval and only the system of equations for delayed neutrons in the interval between pulses. This approximation is known as “the δ -pulse approximation”.

According to the B&S theory (later refined in works by Dubna researchers and by developers of the European pulsed reactor project SORA [18]), the energy of a single pulse Q can be expressed with sufficient accuracy by the following relation:

$$M = \frac{Q}{S} \approx \frac{3.35}{\alpha^{1/2} v \varepsilon_m^{1/3}} \exp\left(\frac{4}{3}B\right). \quad (2)$$

Here, S is the delayed-neutron source preceding the power pulse; α is the parabolic reactivity parameter of the reactivity modulator in the vicinity of its maximum; v is the modulator speed; ε_m is the peak supercriticality with respect to prompt neutrons; and dimensionless parameter $B = \varepsilon_m^{3/2} / (\alpha^{1/2} v \tau)$.

In the steady-state operating regime, the periodicity of the delayed-neutron source intensity S is maintained, which is satisfied under the condition:

$$M_0 \beta_{\text{eff}} \approx T, \quad (3)$$

where T is the reactivity modulation period, and M_0 is the value of the parameter according to equation (2) in the critical mode), corresponding to the critical value of ε_{m_0} . This condition represents the criticality condition of a pulsed reactor and follows from the balance of the delayed-neutron source: accumulation during the pulse equals decay between pulses (assuming that no delayed-neutron source accumulates between power pulses).

The behavior of a pulsed reactor under small reactivity perturbations relative to ε_m on the order of $< 10^{-4} k_{\text{eff}}$ is similar to that of steady-state reactors, in which neutron kinetics is governed by the effective fraction of delayed neutrons. The difference is that in a pulsed reactor this quantity is replaced by the so-called pulse fraction of delayed neutrons β_{pulsed} , which is tens to hundreds of times smaller than the physical delayed-neutron fraction. The pulse fraction of delayed neutrons is related to reactor parameters by the following expression:

$$\beta_{\text{pulsed}} \sim 0.5(\alpha v^2 \tau^2)^{1/3}, \quad (4)$$

where all factors are defined above. Knowledge of these quantities, together with the relationship between pulse energy and reactivity, is sufficient to describe the dynamics of a pulsed reactor under both steady-state and transient conditions. It is noteworthy that the quantity β_{pulsed} is equal to the reciprocal of the number of fission chains occurring during the time the reactor remains supercritical with respect to prompt neutrons:

$$\beta_{\text{pulsed}} = \frac{M}{dM/d\varepsilon} = \frac{\alpha^{1/2}}{2\varepsilon^{1/2}} = \frac{\alpha^{1/2}\tau}{2\alpha^{1/2}t_1} = \frac{\tau}{2t_1}. \quad (5)$$

It is also of interest that even in the absence of power–reactivity feedback, a pulsed reactor operating in equilibrium may *begin to excuse* (!). This occurs when a source of reactivity oscillations appears that is independent of power but has a sufficiently large amplitude on the order of β_{pulsed} . This effect is explained by the nonlinear relationship between ε_m and pulse energy, as can be easily verified.

4.2. Dynamics of a high-power pulsed fast reactor

The influence of the power–reactivity feedback becomes significant in a pulsed reactor when the fuel heating during a single pulse introduces a reactivity change $\Delta\varepsilon$ of the order of β_{pulsed} . Even in the presence of negative feedback ($d\varepsilon/dT < 0$), the behavior of a pulsed reactor differs fundamentally from that of a steady-state reactor. Both theoretical analysis and experimental studies [42] have demonstrated the existence of correlations between the amplitudes of successive power pulses. When the heating per pulse reaches values of $-2\beta_{\text{pulsed}}/(d\varepsilon/dT)$ or higher, the pulsed reactor first exhibits a halving of the pulse repetition period. With a further increase in the magnitude of the feedback, the system transitions to stochastic behavior resembling the Feigenbaum scenario [43]. Figure 16 shows a calculated example for the IBR-2 reactor operating at power levels of 8 MW and above. Naturally, this specific feature necessitates imposing an upper power limit on pulsed reactors.

The above considerations adequately explained the dynamics of first- and second-generation JINR reactors under nominal operating conditions (coolant flow rate and power). However, during the power startup of IBR-2 at power levels of 100–300 kW and above (1983), at low coolant flow rates (liquid sodium), self-oscillatory processes were observed (Figure 17). Self-oscillations of power-pulse amplitudes were detected, including diverging oscillations (which were, naturally, suppressed by the operator). The pulse repetition frequency had no noticeable effect on the fast power-dependent reactivity effect; however, a pronounced dependence on the ratio of reactor power to coolant flow rate was observed, i.e., on the degree of sodium heating in the core. In addition, a reactivity component depending solely on power was identified, characterized by a strong nonlinearity with respect to power.

A detailed analysis of thermomechanical processes in a core of complex design required complicated numerical calculations, for which neither sufficient time nor fast computers were available at that period. The primary task was to bring the reactor into a reliable operating regime, which was successfully achieved: at a sodium flow rate of 100 m³/h and a power of 2 MW, the reactor operated stably for the first 15 years. Nevertheless, operating a reactor without a clear understanding of the details of its dynamic behavior was unsafe, and it became necessary to rely on a “black-box” model with experimentally determined parameters. This was accomplished in the late 1980s by physicists of the nuclear safety group using a mathematical inverse-problem-solving program developed by V. Zlokazov (LIT). The model is based on

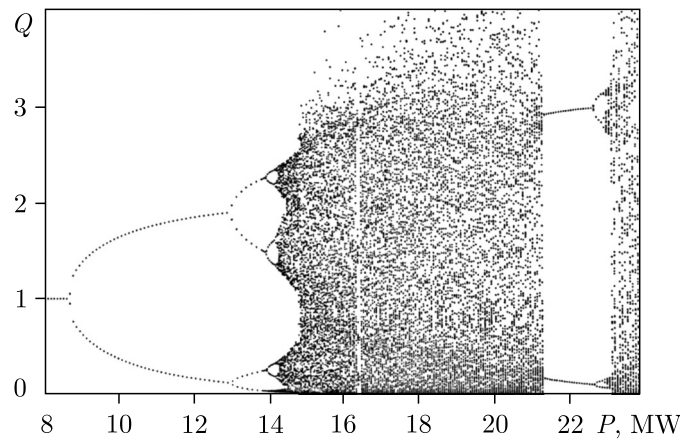


Figure 16. Fluctuations of pulse energies in the IBR-2 reactor (stable operating mode) at high power levels (P , MW), calculation.

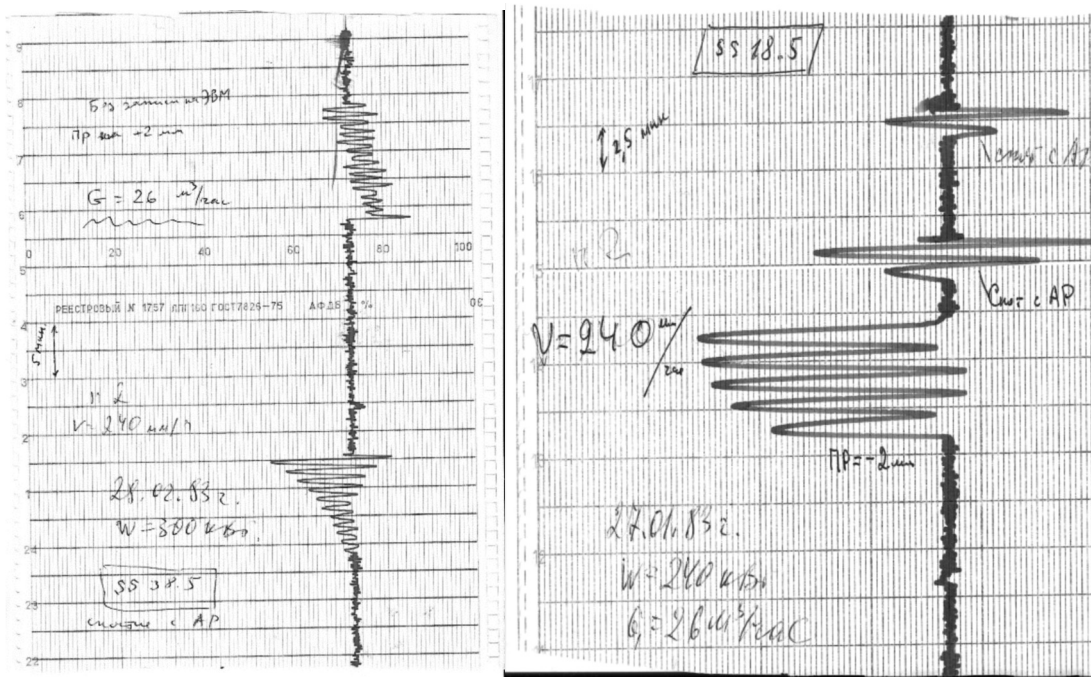


Figure 17. Power self-oscillations in IBR-2: at a power of 360 kW and sodium flow rate of 26 m³/h (left), and at a power of 240 kW with the same sodium flow rate (right).

three fictitious components of the power–reactivity feedback with six parameters (three time constants T_i and three gain coefficients k_i):

$$\rho_{\text{exp}}(t) = \sum_{i=1}^3 \frac{k_i}{T_i} \exp\left(-\frac{t}{T_i}\right). \tag{6}$$

All three components have an exponential time dependence with different characteristic times and amplitudes; two of them are negative (acting to reduce power during a power excursion), while the third is positive (enhancing the reactor power rise). The combined change in the neutron multiplication factor (reactivity) after a unit pulse energy jump is schematically shown in Figure 18. As it was found later, this behavior is essentially the same for both IBR-2 and IBR-2M.

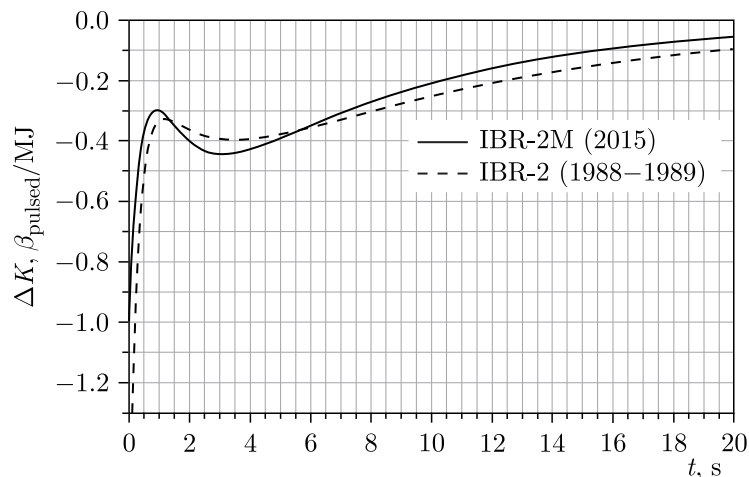


Figure 18. Time dependence of the power feedback after a unit pulse.

Subsequently, IBR-2 (and its modification IBR-2M) was operated exclusively at the maximum coolant flow rate of 100 m³/h. After 10–12 years of operation, self-oscillations began to manifest again. Operating regulations did not permit experimental studies under these conditions, and the search for the physical origins of the positive feedback could only be investigated theoretically. The most plausible explanation appeared to be the transverse bending of fuel assemblies (FAs) under the influence of temperature differences between the assembly walls along the gradient of the power density field. In this case, the resulting positive reactivity contribution $d\rho$ would be determined by both the sodium flow rate and the reactor power:

$$d\rho \sim dx \sim dT \sim a(dP/G - 2PdG/G^2), \quad (7)$$

where dx is the displacement of the FA; dT is the change in the temperature difference between FA walls; and a is the temperature coefficient (calculated or experimental). According to this relation, at a constant coolant flow rate the reactivity should not depend on power; however, experimental observations contradicted this expectation. As a result, the hypothesis of FA bending was rejected at that time. For nearly a quarter of a century, no serious attempts were made to address the problem of self-oscillations. A single internal report issued in 1998 remained unused. . .

When the modernization of IBR-2 to IBR-2M was planned in the mid-1990s, it was assumed that one of the causes of self-oscillations was the presence of a hollow tube in the core center (a vestige of the target intended for the IBR-2 + LINAC-30 booster). However, the opposite occurred: self-oscillations and instability events appeared already after 6–7 years of operation of the IBR-2M reactor. Reactor personnel regularly monitored parameters related to reactor dynamics, with particularly intensive studies of the IBR-2M state after 2018. In 2021, at an average fuel burnup of about 2.5% over the core, the reactor approached instability. The power had to be reduced to 70% of the nominal value. At present, changes in reactor behavior have to be forecast by extrapolating the observed trends in feedback variation over the near-term operating period. Without knowledge of the true physical nature of the power reactivity effect, it is impossible — and irresponsible — to undertake technical or administrative measures that would guarantee safe long-term reactor operation.

In 2022, team of the Sector of the new source and moderator complex began intensive work on the problem of self-oscillations and stability of pulsed reactors, addressing both the NEPTUN project and IBR-2. By the end of 2024, theoretical studies using the experimental data available at that time were completed.

Main results of the study:

1. It proved impossible to associate each of the three feedback components with a specific physical cause. In reality, none of them corresponds to a distinct physical process in the reactor; however, their sum provides a reasonably accurate description of the reactor dynamics and its power feedback.
2. The limitations of the adopted approach are evident. Without understanding the physical origins of the feedback components, it is impossible to predict reactor behavior when operating conditions change (fuel reloading, fuel burnup, design modifications, etc.). Moreover, the theoretically reconstructed power feedback contains at least eight parameters, whereas the three-exponential representation involves only six parameters (Eq. (6)). This implies a significant uncertainty in the reconstruction of the power feedback, which is clearly visible in the analysis of experimental curves: they show no clear trend toward decreasing stability with fuel burnup, although such a trend is observed in practice.

3. It became possible to theoretically estimate the components of the power feedback and to identify their physical origins.
 - Effect No.1. Thermal expansion of plutonium dioxide — both individual pellets and the fuel column as a whole — produces a negative feedback effect.
 - Effect No.2 (the most computationally demanding). A positive reactivity effect caused by bending of the FA cladding due to a temperature gradient directed from the center of the core (in the IBR-2 reactor this effect was approximately 1.5 times smaller). The calculation methodology was developed, and the contribution of this effect to the feedback was quantified [44].
 - Effect No.3 (negative). This effect is associated with the presence of elastic petals in the upper part of the FA casing, provided in the design to prevent contact between the claddings of neighboring FAs. These petals are at the temperature of heated sodium; therefore, during transient sodium temperature changes, an effective “swelling” of the core occurs.
 - Effect No.4. Dynamic bending of fuel element claddings. Depending on the design, this effect can contribute either positively or negatively to reactor dynamics (a more detailed discussion is given below). It manifests itself as increased reactivity fluctuations; its influence on stability has not been detected yet.
 - Effect No.5. Fuel pellet hanging-up (jamming), which always contributes positively but manifests itself only at significant fuel burnup [45].

The identified feedback components do not coincide with those previously assumed on the basis of the three-exponential dynamic model. For example, the exponential function describing the positive feedback component has its maximum absolute value at time zero, which is physically absurd — it is difficult to imagine a real physical phenomenon behaving in this manner. Likewise, there is no reasonable explanation for the fast component of the negative feedback. Nevertheless, the combined power feedback curve of the first three effects is close to that experimentally reconstructed using the black-box model: it exhibits two extrema within the time window of 0–4 s, as shown in Figure 19. A detailed comparison will become possible after estimating calculation uncertainties.

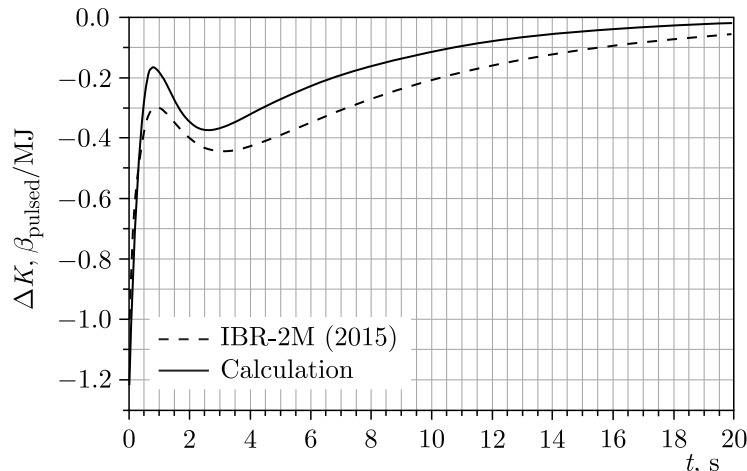


Figure 19. Comparison of calculated and experimental power feedback.

Due to the format limitations of the present article, it is not possible to describe in detail the methodology and results of theoretical (partly experimental) studies of all five effects, including their influence on the dynamics and stability of pulsed reactors. Below, we briefly discuss only two of them, which play a decisive role in the dynamics of both the IBR-2M reactor and the NEPTUN reactor project.

4.3. The influence of dynamic bending on dynamics of a pulsed fast reactor

Dynamic bending refers to the nonstationary transverse deformation of fuel elements (FEs) in a pulsed reactor under the action of thermoelastic and inertial forces. Its key feature is that the response of FE bending to periodic and pulsed temperature variations differs fundamentally from that under steady-state conditions. Under stationary power generation, FE bending is directed toward the core center when both ends of the FE are sufficiently rigidly fixed, and away from the center when one end is free (Figure 20).

In the first case, the reactivity effect is positive, thereby reducing reactor stability; in the second case, stability is enhanced. Under cyclic power generation (pulsed reactor operation), the situation is far less straightforward. After a power pulse, a bent fuel element begins to oscillate. Depending on the relationship between the natural oscillation frequencies and the reactor pulse repetition frequency, at the moment of the next power pulse the FE may occupy different positions relative to its initial (or steady-state) position. As a result, its oscillations may either be amplified or damped, even with an unchanged fixing scheme. At sufficiently large deflections, fuel elements may collide with each other, which further alters their dynamics. This is why transverse bending in a pulsed reactor is referred to as “dynamic”.

In addition to the effects described above, another factor must be taken into account that enhances reactor fluctuations due to dynamic bending. As discussed in Section 4.1, oscillations of external reactivity in a pulsed reactor are equivalent to reactivity insertion. Thus, irrespective of the direct reactivity effect of bending itself, an additional “quasi-reactivity” arises as a consequence of periodic pulsing, which further “excites” the reactor.

The methodology for calculating the influence of dynamic bending on transient processes in a pulsed reactor is based on the point kinetics B&S model with delayed neutrons for a pulsed reactor, formulated for energy pulse sequences Q_i and delayed neutron precursor sources. To this system are added equations for the fuel temperature T_i , the FE cladding temperature T_s , the thermoelastic equation for the cladding, and relations for calculating feedback reactivity from transverse R_{tr} and axial R_{ax} displacements of the fuel and cladding. In the simplest case, when only the fundamental harmonic of cladding oscillations is considered, the equations take the form

$$\begin{cases} T_i = (T_{i-1} + Q_{i-1}T_0) \varphi, \\ T_s(t) = \sum_{l=i-1}^0 T_{s0} \left(\frac{1}{\nu} \cdot (i-l) + t' \right) \cdot Q_l, \\ \ddot{x} + \frac{2}{\tau} \dot{x} + (2\pi\nu)^2 x = AT_s(t), \end{cases} \quad (8)$$

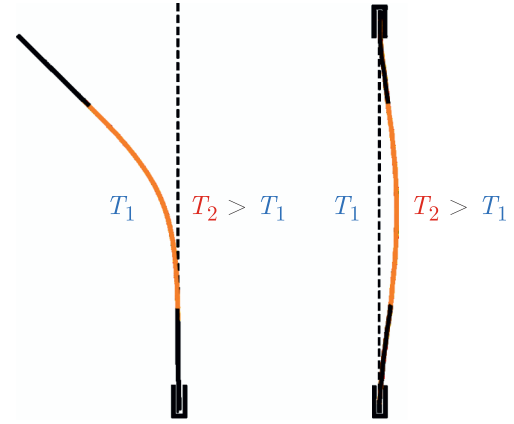


Figure 20. Direction of fuel element bending depending on the fixing scheme. The fuel region is shown in orange.

where φ is the temperature decay factor over one pulse period (a quantity close to unity); ν is the pulse repetition frequency; x is the axial thermal deformation of the cladding; and τ is the damping time of cladding oscillations. The parameter A determines the magnitude and direction of bending due to a unit pulse energy: a positive value corresponds to bending toward the core center, i.e., an increase in reactivity. Subscripts “0” denote equilibrium operating parameters (initial conditions).

The most complex and time-consuming part of the analysis is the calculation of the reactivity induced by bending, which is represented as the sum of partial reactivity contributions R_k from the first five harmonics of the transverse nonstationary deformation of the fuel element y_k at the moment of each i -th power pulse (where k is the harmonic number):

$$\rho_r = \sum_k y_k R_k. \quad (9)$$

In the general case, the equation of motion can be written in operator form $y_{ki} = D(y_{ki-1})$. The operator D is defined by the dynamic thermoelastic equations — second-order differential equations that are solved numerically with continuous time integration using a time step of 10^{-4} s.

All parameters and functions, except $T_i(t)$ and $T_s(t)$, are determined in advance from the FE design and its fixing scheme. The method for calculating R_k (reactivity coefficients for the k -th harmonic of transverse deformation), as well as the corresponding eigenfunctions and eigenvalues, is performed prior to the dynamic analysis and is described in [46].

Dynamic bending affects the character of power oscillations in a pulsed reactor whenever sufficient freedom for transverse displacement of fuel elements exists. A characteristic coupling between displacement and reactivity in IBR-type pulsed reactors exceeds $10 \beta_{\text{pulsed}}$ per 1 mm. Accordingly, an average FE displacement of only $10 \mu\text{m}$ along its length results in a change in pulse energy exceeding 10%. In practice, for almost any fixing scheme and arrangement of fuel elements in the core, dynamic bending acts as an active factor in the dynamic process. It can be significantly suppressed only at sufficiently high-power levels, when fuel elements within a fuel assembly become “tightly packed”. Figure 21 presents a characteristic example of pulse dynamics in a pulsed reactor in the presence of the dynamic bending effect. The growing

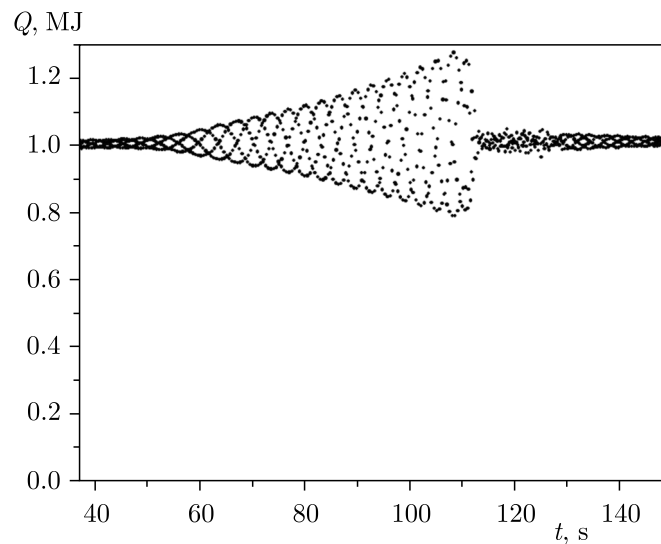


Figure 21. Dynamic process with stabilization of pulse oscillations due to inelastic collisions between fuel elements.

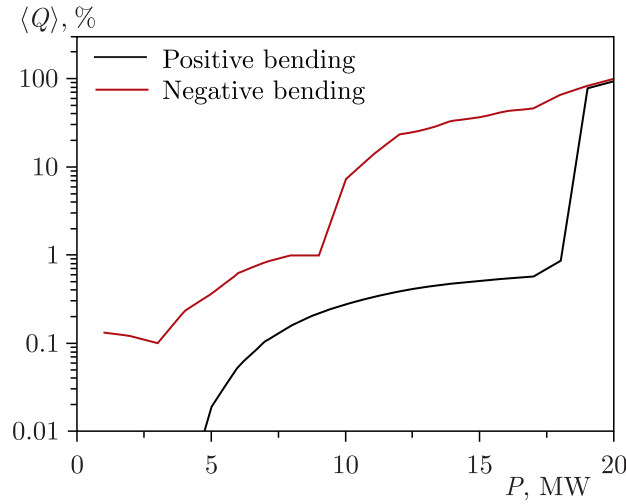


Figure 22. Pulse energy fluctuations in the NEPTUN reactor project for two types of fuel element fixing.

oscillations indicate that, during this period, collisions between fuel elements are either rare or elastic; at large deflections and with inelastic interactions, the oscillations are damped.

In the NEPTUN project, the currently relevant core configuration is a pin-by-pin (assembly-free) arrangement. The first natural harmonic of FE oscillations in NEPTUN is 8.5 Hz, while the reactor pulse repetition frequency is 10 Hz. According to calculations based on the dynamic model discussed above, pulse energy fluctuations are small at powers below 16 MW for the case of FE fixing corresponding to $A > 0$ (Figure 22). For $A < 0$, the situation is significantly worse. This seemingly counterintuitive result is explained by the phase shift between the mechanical oscillator and power generation, as discussed above. It clearly demonstrates the critical importance of thorough analysis of dynamic processes in pulsed reactors.

4.4. The influence of static fuel assembly bending on dynamics of a pulsed fast reactor

Static bending of FAs arises due to nonuniform power generation within the reactor core. As a consequence, heat transfer within an assembly — from the fuel elements to the adjacent FA walls — differs across the assembly cross section. The FA wall located closer to the core center is heated more strongly. As a result, the bending is directed toward the core center (Figure 20), and the associated reactivity contribution is positive.

In [44], a numerical calculation of transverse FA deformations for the IBR-2M reactor was performed, and their influence on reactivity and reactor dynamics was evaluated. The corresponding feedback reactivity is shown in Figure 23.

The methodology for analyzing the dynamics of a pulsed reactor with two-component feedback (axial fuel expansion and transverse FA deformation) is based on a system of recurrent relations [47]:

$$\begin{cases} Q_i = S_i M (\varepsilon + R_i), \\ S_i = \sum_j c_{ji} \lambda_j, \\ c_{ji} = (c_{ji-1} + Q_{i-1} \beta_j \nu) \exp(-\lambda_j T), \\ R_i = \beta_{\text{pulsed}} \sum_{k < i} Q_k (x \rho_f (T[i-k] + \rho_b (T[i-k]))), \end{cases} \quad (10)$$

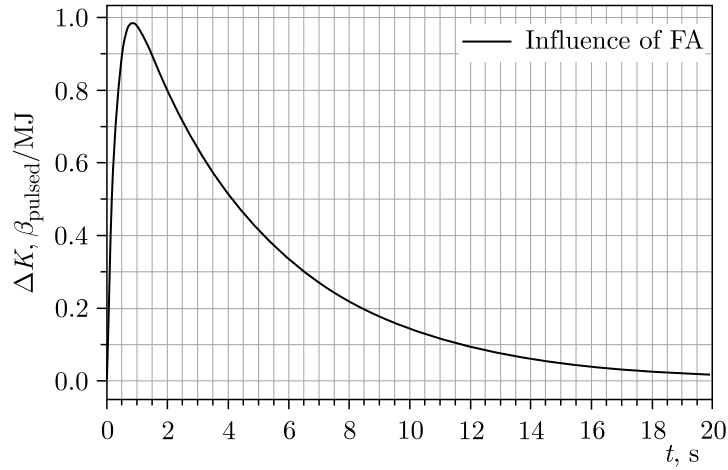


Figure 23. Reactivity change after a 1 MJ pulse due to fuel assembly bending.

where $M(\varepsilon)$ is the multiplication factor, calculated either using approximate relations [48] or specified by a lookup table; R_i is the feedback reactivity; c_{ji} is the number of delayed neutron precursors of group j (eight-group approximation) at the i -th pulse; λ_j is the decay constant of precursors of group j ; β_j is the fraction of delayed neutrons of group j ; ν is the average number of neutrons per fission; T is the reactor pulse period; β_{pulsed} is the impulsive fraction of delayed neutrons; ρ_f is the reactivity change due to thermal expansion of the fuel [49]; x is the burnup factor; and ρ_b is the reactivity change due to transverse FA deformation [44].

As fuel burnup progresses, a weakening of feedback is observed. Therefore, in system (10) a parameter x is introduced for the negative feedback component, which varies from 1 (no burnup) to 0 (absence of fuel-related feedback).

In [49], the influence of burnup on the dynamics of the IBR-2 reactor was studied using the two-component feedback approximation. For the nominal power of 2 MW, the system remains stable for $x > 0.69$; for $x < 0.69$, the system becomes unstable (Figure 24).

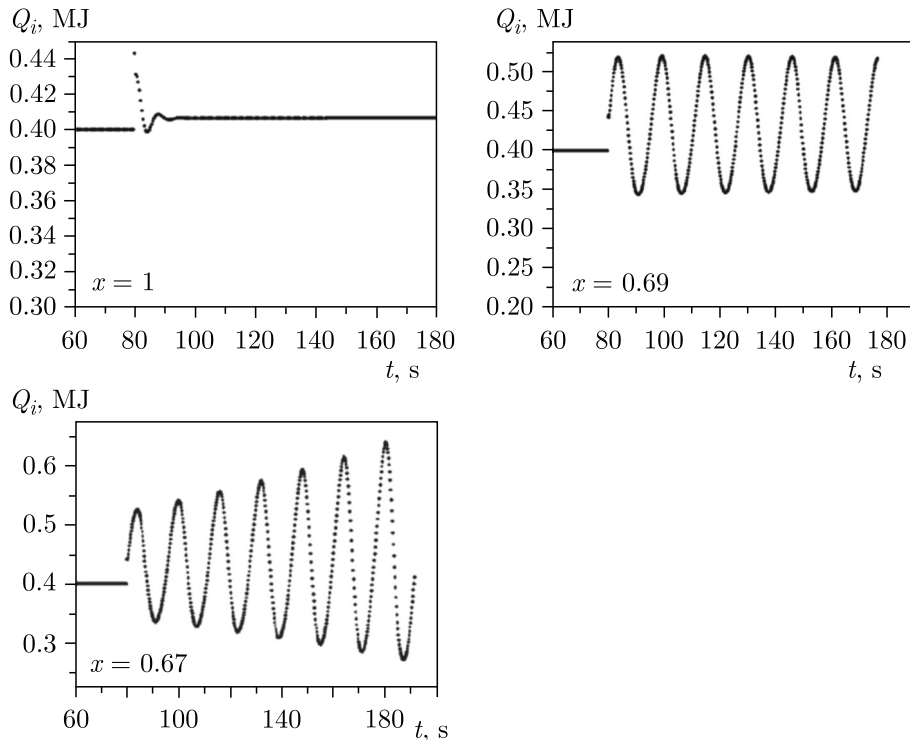


Figure 24. Power pulse dynamics for different values of x [49].

This methodology makes it possible to study and evaluate the influence of individual physical processes in the core on pulse stability. Representing power feedback as a sum of partial reactivity contributions from different effects is more adequate for reactor dynamics studies, since it is based on well-defined physical processes in the core, unlike the three-exponential representation (6).

It should be noted that during the calculation of the FA bending effect, an interesting feature was revealed: the actual bending of the FA shroud occurs in a plane rotated relative to the direction of the power density and temperature gradient. This is caused by the influence of spacer wire winding and sodium flow rotation. The current result, $+4 \beta_{\text{pulsed}}/\text{MW}$ at any power level and any burnup, is approximately 1.5 times higher than earlier analytical estimates.

5. Third generation. The NEPTUN reactor

5.1. Limitations on neutron flux

The IBR-2 reactor occupies a unique position among neutron sources worldwide. It is the only periodically pulsed reactor based on prompt fission, and in terms of peak neutron flux it remains among the world's leading sources. The top positions are currently held by accelerator-driven spallation facilities employing GeV-class proton beams — specifically, STS (the second target station of SNS, Oak Ridge, USA) and JSNS (Ibaraki, Japan) — where peak neutron fluxes at the surface of the external moderator reach $\Phi_p^T \sim (5-6) \cdot 10^{15} \text{ cm}^{-2} \cdot \text{s}^{-1}$. For comparison, IBR-2M provides $\sim 3 \cdot 10^{15} \text{ cm}^{-2} \cdot \text{s}^{-1}$. The upcoming European Spallation Source (ESS, Lund, Sweden), operating with a 1.25 GeV proton accelerator and a 2.5 MW beam power, is expected to achieve similar values. These represent the upper technological limit for accelerator-based neutron sources. The question arises: is it feasible for a pulsed fission reactor to exceed this level?

The time-averaged thermal neutron flux density on the surface of the water moderators at IBR-2, $(5-10) \cdot 10^{12} \text{ cm}^{-2} \cdot \text{s}^{-1}$, is significantly lower than that of the best spallation sources. For comparison, ESS is expected to achieve $\sim 10^{14} \text{ cm}^{-2} \cdot \text{s}^{-1}$. Furthermore, the pulse duration of IBR-2, about 300 μs , is essentially fixed, whereas accelerator-driven sources are capable of generating substantially shorter pulses (down to $\sim 20 \mu\text{s}$), which provides superior energy resolution in neutron spectrometry. Optimization studies of IBR-2 indicate that a significant increase in average power, and thus neutron flux, is practically unattainable for plutonium-based fuel. Fundamental limitations arise both from the stability issues discussed previously and from the thermal-shock effect (addressed below). Defining the development strategy for next-generation neutron sources is now a key issue for JINR, particularly given the finite operational lifetime of IBR-2 in the coming decade. This section is devoted to that consideration.

In sources of significant size, such as multiplying targets and pulsed reactors, where the migration length of fission neutrons is much smaller than the characteristic dimension of the core–target system, the thermal neutron flux density in the moderator is determined not so much by the total power as by the volumetric density of neutron generation in the region adjacent to the moderator $Q_f(x)$:

$$Q_f(x) = \int \Sigma_f(E) \Phi(E, x) dE = \bar{\Sigma}_f \cdot \Phi(x) = W_{sp}(x) \cdot 3.1 \cdot 10^{13}, \quad (11)$$

where $\Phi(E, x)$, $\Phi(x)$ are the differential and total neutron flux densities, $\text{cm}^{-2} \cdot \text{s}^{-1}$; $\bar{\Sigma}_f$ is the macroscopic fission cross section averaged over the energy spectrum, Q_f is the volumetric density of fissions, and W_{sp} is the specific power density, MW/l; all quantities refer to a region

of the core near the neutron moderator. The thermal neutron flux density at the outer surface of the moderator — the most important characteristic of a pulsed source for experiments on extracted beams — is approximately proportional to the neutron flux density in the core at the boundary with the moderator:

$$\Phi_{\text{th}}(x) \approx a\Phi(x), \quad (12)$$

where the coefficient a is determined by the “core–moderator” geometry and by Fermi’s slowing-down law for neutrons. Depending on geometry, $a \approx 0.1\text{--}0.2$. Relations (11) and (12) define the upper limit of the thermal neutron flux in pulsed sources for a given average power density:

$$\Phi_{\text{th}}(x) = \frac{W_{sp}(x)}{\sigma_f} \alpha \cdot 1.23 \cdot 10^{16}. \quad (13)$$

Here, γ is the density of fissile material, kg/l; σ_f is the microscopic fission cross section, b. The calculated dependence of the angular thermal neutron flux (2π -equivalent) from the surface of an external comb-type water moderator on the core volume — taking into account the reduced contribution of the central core regions to the neutron flux — is shown in Figure 25. Modern fast-neutron reactor technology with ceramic fuel (BR-10, BOR-60, MBIR) allows one to reach no more than 0.25–0.5 MW/l (depending on core size), whereas in reactors operating on resonance neutrons, such as SM-3 and PIK, the volume-averaged specific power density reaches 2 MW/l. The remaining parameters in Eq. (13) also have their own limits imposed by reactor design. In particular, the fuel density in the core of a pulsed reactor or booster (parameter γ) cannot be substantially reduced because of the detrimental effects of thermal shock during pulsed heating of the fuel, according to the relation

$$\Delta T = \frac{W_{sp}(x)}{\gamma n c_m}, \quad (14)$$

where n is the pulse repetition frequency and c_m is the heat capacity of the fuel, MJ/(kg · K). Rapid heating of nuclear fuel beyond the permissible level leads to premature degradation of the fuel kernel and/or damage to the fuel element cladding.

In fast plutonium reactors, the fission cross section σ_f remains in the range of 1.5–2 b over a broad neutron energy interval from 10 keV to 4 MeV. In self-quenching pulsed fast reactors with metallic fuel operated at the Sarov and Snezhinsk research centers, the limiting

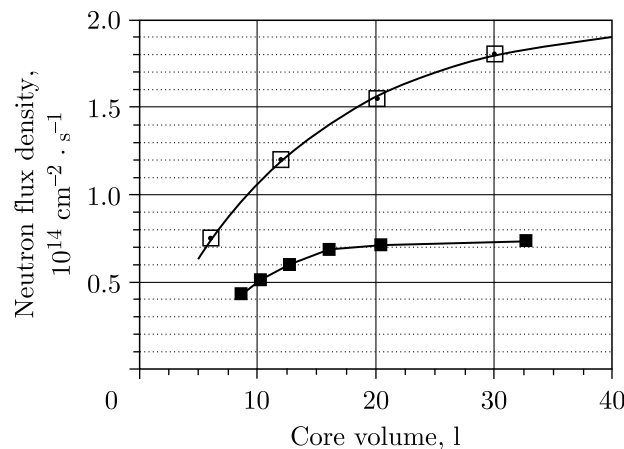


Figure 25. Dependence of the neutron flux density at the surface of a comb-type water moderator on the reactor core volume; $W_{sp} = 0.33$ MW/l. \square — fast reactor cooled by liquid sodium; \blacksquare — plutonium resonance-neutron reactor cooled by water.

values of pulsed temperature rise reach several hundred degrees. For repeated bursts in a periodically pulsed reactor, however, the temperature change during the short pulse duration of 200–300 μs — determined by relation (14) — must be at least an order of magnitude lower because of material fatigue. Experimental and theoretical studies of the thermal shock effect performed during the development of IBR-2 allow one to conclude that the temperature rise per pulse in a solid ceramic fuel kernel should be limited to 40–50 K. Under this condition, for plutonium dioxide fuel at a pulse repetition rate of $n = 10$ Hz, the following limitation on the maximum neutron flux follows from relations (13) and (14):

$$\Phi_{\text{th}} < \frac{\Delta T n}{\sigma_f} c_m \cdot 0.48 \cdot 10^{13} \approx (3-6) \cdot 10^{13}. \quad (15)$$

This value is lower than the flux corresponding to the limit imposed by specific power density. For a reactor using neptunium nitride fuel, owing to the threshold character of fission (Figure 26), the fission cross section averaged over the entire spectrum (from 0.1 to 4 MeV) is 1.5–2 times lower than that of plutonium, which increases neutron leakage at equal power density. At the same time, the higher density of neptunium nitride reduces fuel heating at the same specific power. Together, these factors increase the limiting thermal neutron flux in a neptunium-based reactor by approximately 20–30% compared with a plutonium core.

Thus, a thermal neutron flux density of about $10^{14} \text{ cm}^{-2} \cdot \text{s}^{-1}$ in fission-based pulsed sources represents the technological limit of nuclear engineering for the first half of the XXI century. In the above discussion, the neutron flux from a flat water moderator of optimal dimensions has been considered; for reactors with a beryllium reflector, the flux may be higher by a factor of 1.5–2. This barrier could be overcome by transitioning to long-patented concepts involving liquid circulating fuel or uranium cyclotron-boiler-type systems, which could increase the flux by approximately an order of magnitude [50]. However, such an approach appears questionable: the construction cost would likely be no lower than that of accelerator facilities with comparable capabilities, and, moreover, society is currently not prepared for such breakthroughs. At the same time, for a non-fissile tungsten target, the cyclotron-boiler principle is applicable; at the ESS target station, for example, the rotating target consists of 33 tungsten segments.

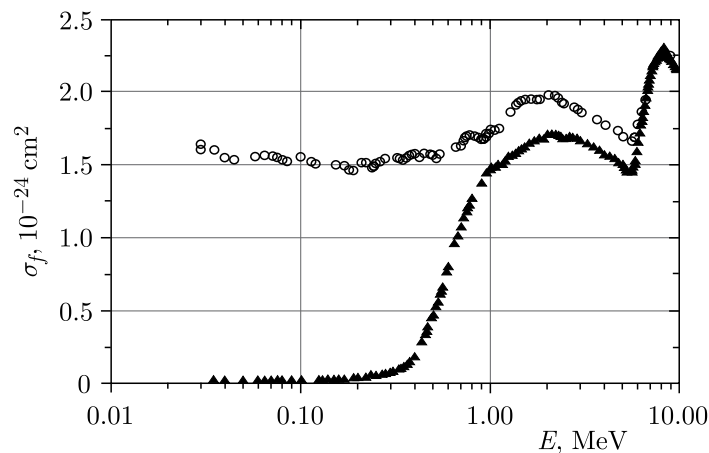


Figure 26. Microscopic fission cross sections of Pu-239 (\circ) and Np-237 (\blacktriangle) in the fast-neutron energy region.

5.2. The NEPTUN reactor

Already at the design stage of IBR-2 in the 1960s, the ultimate capabilities of a pulsed fast reactor for condensed-matter physics research were investigated. It was shown that the best parameters of thermal-neutron beams are provided by a fast-neutron reactor with a core volume exceeding 15–20 l and an average thermal power of at least 10 MW [17]. At that time, the only operating pulsed reactor was IBR — a low-power (1–3 kW), air-cooled reactor with metallic plutonium fuel, commissioned in Dubna in 1960. It was considered risky to proceed directly to a reactor with limiting loads exceeding those of IBR by several orders of magnitude, and IBR-30, with a power of 20 kW, became the successor to IBR. By that time, sufficient and successful experience had been accumulated at IPPE with fast reactors cooled by liquid sodium, such as BR-5 and BR-10 with powers of 5 and 10 MW, respectively. This experience made it possible to initiate the project of a 4-MW pulsed reactor using the technology of these reactors. As a result, the operating limit of IBR-2, commissioned in 1984, became a power of 2 MW. Nevertheless, for more than 30 years, the IBR-2 and IBR-2M reactors have been — and to some extent still remain — the highest-flux sources of thermal neutrons for experiments on extracted beams, providing a peak neutron flux density at the surface of the external moderator of up to $6 \cdot 10^{15} \text{ cm}^{-2} \cdot \text{s}^{-1}$ and an average flux density of up to $10^{13} \text{ cm}^{-2} \cdot \text{s}^{-1}$.

In the NEPTUN design (Figures 27, 28), technical solutions characteristic of the IBR and IBR-2 reactors are largely retained; however, several innovations are introduced that make it possible to reach limiting parameters [51], namely:

- Neptunium-237 is used as nuclear fuel instead of plutonium;
- Reactivity modulation is based on the principle of removing hydrogen-containing material from the core (instead of withdrawing a reflector);
- Beryllium is used as a stationary reflector;
- Slow-neutron beams are extracted tangentially to the boundaries of the core.

The effects of each of these factors are discussed in detail below.

The core is located in two identical stainless-steel vessels, between which the rotor of the reactivity modulator passes. The core consists of an assembly of densely packed fuel elements, in which the rapidly developing chain fission reaction of neptunium-237 nuclei takes place.

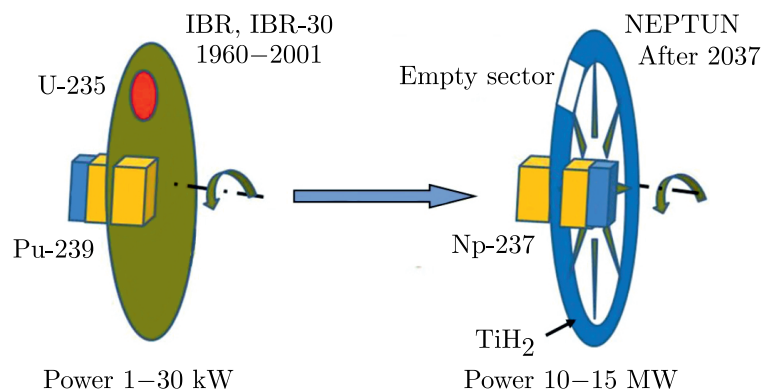


Figure 27. Illustration of the pulse-generation principle in the IBR and NEPTUN reactors: continuity and differences.

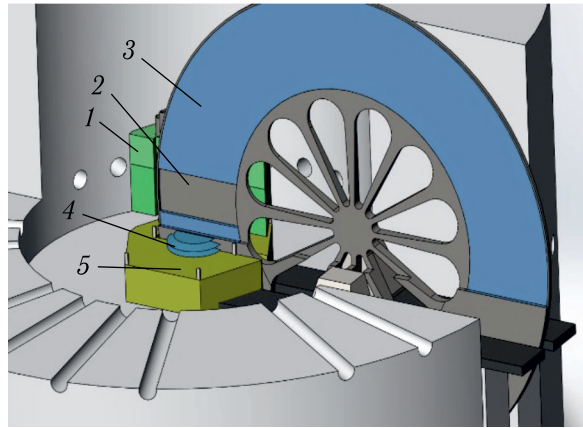


Figure 28. Schematic layout of the NEPTUN reactor with shielding and neutron beam extraction. 1 — one of the two halves of the core with a nickel reflector; 2 — empty sector in the reactivity-modulator disk; 3 — titanium hydride; 4 — water neutron moderator; 5 — beryllium reflector-moderator.

The fuel-element kernel, 16 mm in diameter, is made of neptunium nitride and is placed in a steel cylindrical cladding with a diametral gap of 0.4 mm to compensate for nitride swelling during burnup. Over a reactor campaign of 15–20 years, the swelling is expected to reach 6–7.5% of the fuel volume at a temperature of 1300 K (corresponding to a burnup of 4–5% of heavy atoms). The gap between the kernel and the cladding is filled with sodium, which remains in the liquid phase owing to the elevated pressure in the fuel element gas plenum.

Heat removal from the fuel elements and the nickel stationary reflector is carried out by liquid sodium using a two-loop scheme similar to that of the IBR-2 reactor. Unlike IBR-2, the lowest point of the primary loop is located within the core vessel, which prevents sodium loss in the event of a rupture of the supply pipe. Coolant circulation is provided by electromagnetic pumps. The operating temperature of sodium in the primary loop is 290–450 °C, and the coolant flow rate at a power of 10 MW is 180 m³/h.

In order to reduce the critical mass, the fuel-element lattice pitch is uniform over the entire core cross section. Another characteristic difference from IBR-2 is the rigid fixation of one (or both) ends of the fuel-element rods in the support plate. This improves the dynamic properties of the reactor (see Section 4.3) and ensures power stability.

For the maximum attainable volumetric fraction of nitride, 72–73%, the calculated critical loading of the neptunium reactor is about 500 kg. The corresponding core volume is approximately 50 L.

The modulator is designed as a rotating disk with a diameter of 3.4 m, along the periphery of which titanium hydride with a density of up to 3.7 g/cm³ is placed in the form of radial sectors. In one of the sectors, titanium hydride is replaced by a void. When this empty sector enters the core region, the neutron multiplication factor increases as a result of spectral hardening. The rotational speed of the modulator rotor is 10 rps, and the effective linear velocity is about 90 m/s.

Titanium hydride is radiation-resistant, well studied, and widely used in the biological shielding of nuclear-power installations. Its high hydrogen content is retained up to temperatures of 500 °C. The modulator is air-cooled. The thermal and radiation loads on the titanium hydride in the sectors adjacent to the void are rather high — up to 3.5 W/cm³ at a reactor power of 10 MW. Therefore, in order to extend the service life of the modulator, the disk is

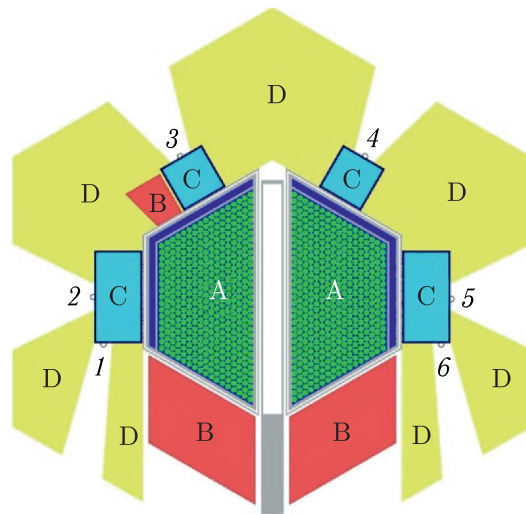


Figure 29. NEPTUN reactor layout, transverse section. A — core consisting of two trapezoidal halves (the empty sector of the reactivity-modulator disk is located between them); B — nickel reflector with control and protection system elements; C — water moderators of fast neutrons; D — beryllium reflector-moderator; 2, 3, 4 and 5 — surfaces for radial neutron beam extraction; 1 and 6 — tangential beams.

designed so as to allow periodic replacement of the hydride sectors that are located near the core during power pulses with more remote sectors.

The use of such a modulator provides a deeper reactivity modulation than a movable reflector (approximately by a factor of 2). The background reactor power is expected to be 2.5–3% of the average power.

Beryllium as a reflector is particularly effective for reactors with a neptunium core. Owing to the threshold nature of fission, reflected neutrons do not induce fission and therefore do not lengthen the power pulse. At the same time, the thermal neutron flux density from the water moderators in the geometry shown in Figure 29 increases due to neutrons reflected from beryllium toward the moderators. The gain in flux relative to a nickel reflector amounts to a factor of 1.5–2.

5.3. Why neptunium?

The principal distinguishing feature of the Np-237 isotope, as compared with conventional nuclear compositions based on U-235 and Pu-239, is the threshold character of its fission cross section (Figure 26). Importantly, the effective fission threshold is approximately 0.4 MeV, which is 0.2 MeV lower than the fission threshold of U-238. This makes it possible to achieve criticality at a sufficiently high density of neptunium nuclei [52, 53]. It is known that for the α -phase of metallic Np-237 with a density of 20.45 g/cm³, $k_{\infty} = 1.638$, and that a bare sphere of metallic neptunium of the same density has a critical radius of 8.864 cm and a critical mass of 59.7 kg.

What are the consequences of such a fission-cross-section behavior? There are at least three important implications.

- First, the prompt neutron generation lifetime τ in a neptunium core is significantly shorter than that in a plutonium core. For example, in the operating fast research reactor IBR-2, $\tau = 65$ ns; in reactors operating on intermediate neutrons it reaches several microseconds;

whereas in a neptunium reactor τ lies in the range of 3–10 ns, depending on the volumetric density of nuclear fuel in the core. This factor enables a shorter burst of fast (and consequently thermal) neutrons in pulsed-reactor operation, since the reactor power pulse duration is proportional to the square root of the neutron generation lifetime.

- Second, the effective delayed-neutron fraction β_{eff} turns out to be noticeably lower than that for plutonium, for which in IBR-2 β_{eff} is $2.16 \cdot 10^{-3}$. This is because delayed fission neutrons have energies from 0.2 to 0.8 MeV, with an average energy of about 0.4 MeV — precisely equal to the fission threshold energy of Np-237 [54–56]. As a result, despite the physical delayed-neutron fraction of neptunium being about $4 \cdot 10^{-3}$, its effective value in the NEPTUN core is only $1.1 \cdot 10^{-3}$. The low value of β_{eff} determines a low background power N_{bg} between pulses, which is estimated to be 2–3% for NEPTUN, compared with 7–8% for IBR-2M, according to the relation

$$\frac{N_{bg}}{N} = \beta_{\text{eff}} / |\varepsilon|, \quad (16)$$

where N denotes the average core power and ε is the degree of subcriticality of the reactor in the background state.

- The third important consequence of the threshold character of neptunium fission is the possibility of using neutron-moderating materials in the reactivity modulator. Moderation on hydrogen nuclei (with a high scattering cross section — about 4 b for the fission spectrum — and an average neutron energy loss of about 50% per collision) leads to a rapid removal of neutrons from the fission region of neptunium. In essence, hydrogen in a neptunium core acts as a neutron absorber (more precisely, as an absorber of “neutron value”). The removal of hydrogen-containing material (for example, titanium hydride) from the core of a neptunium reactor produces a reactivity change comparable to the insertion of fissile material. Such an effect cannot be achieved by moving an equivalent volume of reflector material.

In addition to the threshold nature of fission, neptunium fuel possesses another remarkable property: during reactor operation, the neutron multiplication factor does not decrease with neptunium burnup, as is typical for uranium- and plutonium-based reactors, but instead increases (Figure 30). The explanation is straightforward. Neutron capture by an Np-237 nucleus produces the β -radioactive Np-238 nucleus, which decays with a half-life of 2.12 days into

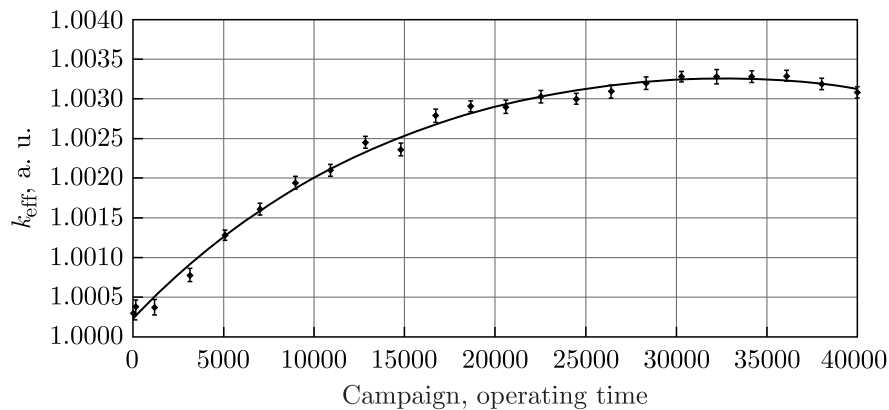


Figure 30. Change in the neutron multiplication factor (% of k_{eff}) in the NEPTUN reactor as a function of operating time.

Pu-238. The latter is a non-threshold fissile isotope with fission properties significantly superior to those of Np-237. Since neutron capture by Np-237 occurs at nearly the same rate as fission, the neutron multiplication factor in a neptunium reactor increases with burnup, in contrast to the familiar decrease observed in uranium or plutonium reactors.

A substantial body of literature is devoted to the study of the mechanical and thermo-physical properties of neptunium and its alloys, see, for example, [57–59]. Actinide nitrides, and neptunium nitride in particular, exhibit highly attractive properties for nuclear fuel applications, including high density and good thermal conductivity. The properties of neptunium nitride have been actively investigated over the past two decades in connection with the problem of radioactive-waste transmutation. On the one hand, neptunium belongs to the most abundant nuclear wastes; on the other hand, it is itself a potential nuclear fuel component in plutonium-based compositions. In this area, the work of Japanese researchers is particularly well known [60–62].

The use of neptunium nitride specifically in a pulsed reactor serving as a neutron source for experiments on extracted beams is especially attractive. A reactor core based on neptunium oxide, owing to its lower density, would be significantly larger, and to achieve the same neutron flux would require increasing the reactor power by a factor of two to three compared with a nitride-based reactor. This is because the neutron flux of a research reactor for extracted-beam experiments is determined not by the total thermal power, but by the specific power density (see Section 5.1). In addition, nitrides possess substantially higher thermal conductivity, which makes it possible to operate at higher specific power densities in a core with large-diameter fuel elements.

How available is neptunium? Np-237 is an artificial isotope with a half-life of $2.14 \cdot 10^6$ years and accumulates as a by-product during the operation of power reactors, as a result of the β -decay of U-237 (half-life 6.7 days). The latter is formed in fast reactors via the $(n, 2n)$ reaction on U-238 or through double neutron capture on U-235 followed by U-236 in thermal reactors. Np-237 constitutes one of the most significant wastes of the nuclear-power industry. A single VVER power unit produces up to 13 kg of neptunium per year. Radiochemical methods for separating Np-237 are currently well established. The global inventory of accumulated Np-237 continues to grow and is presently measured in tons (exact figures are unknown to the authors). Thus, the task of obtaining the 300–600 kg of Np-237 required for constructing a research reactor is, in principle, solvable.

At present, the only practical application of Np-237 is the production of Pu-238, an essential long-lived power source for space missions. In the monographs by V. F. Kolesov [63], the use of Np-237 as fuel for the inner core (AZ1) of a two-section booster reactor with an outer U-235 core (AZ2) is discussed in detail, aimed at creating an ultra-high-power fast-neutron source with the so-called valved neutron coupling between the sections. It is shown that AZ1 in such a system can operate both in booster mode (with a linear electron accelerator) and in the mode of a self-quenching, aperiodic pulsed reactor. Such a two-zone system is effective for irradiation experiments or for the creation of nuclear-pumped lasers [64]; however, for the generation of extracted pulsed neutron beams it offers no advantages over a single-zone booster or a pulsed neptunium reactor.

6. Conclusion

Let us summarize the results. 65 years of experience in operating pulsed reactors at FLNP have demonstrated the high (by world standards) effectiveness of the scientific and applied research carried out using these facilities. The IBR reactor was the world's first pulsed reactor,

followed by first- and second-generation reactors with neutron fluxes on extracted beams almost four orders of magnitude higher. Experience gained in operating these high-intensity neutron sources revealed a characteristic feature of pulsed fast reactors. Let us clarify the statement.

In the 1980s, a unique second-generation nuclear reactor, IBR-2, was constructed. While it possessed good output parameters, it also exhibited a serious drawback: during operation, spontaneous power oscillations arose, which under certain conditions could lead to reactor runaway. To prevent this, the reactor power had to be reduced. At IBR-2, these problems began to manifest themselves after 10–12 years of operation starting in 1984. Prior to shutdown for modernization in 2006, the reactor was operated at reduced power. An attempt was made to improve IBR-2 during modernization. However, the “improved” IBR-2M reactor required power reduction already 5–6 years after the start of operation in 2012. By 2021, before the reactor was shut down for repair, a power reduction by nearly a factor of 2 was under consideration. At present, safe operation of the reactor is possible at a power of no more than 1.4 MW.

Following a thorough analysis of operational experience and theoretical studies, the cause of the unstable self-oscillations was identified. They are due to positive feedback arising from transverse bending of fuel assemblies. The degradation of reactor dynamics with fuel burnup is most likely caused by a decrease in the heat capacity of plutonium dioxide with burnup, as well as by the hanging-up (jamming) of fuel pellets in the central region of the core. It is now evident that any attempts to reproduce the basic design concept of IBR-2 with fuel assemblies in the core encounter, at a minimum, the problem of unstable power-pulse oscillations, for which no solution has yet been found.

An alternative may be the NEPTUN reactor with pin-type fuel loading or in the form of two mono-zones. A traditional core configuration with fuel assemblies is also not excluded; however, in this case, no engineering solution has been found yet that would eliminate power oscillations. A reactor of the NEPTUN type can be realized as a dual-purpose source — for studies of solid and liquid structures, as well as for nuclear and fundamental physics (JINR booklet *Superbooster NEPTUN*, Dubna, 2018). Such designs are free from the instability problem and possess neutron-physical parameters (neutron flux density on extracted beams, background power, pulse duration, and operating lifetime without refueling) that are an order of magnitude superior to those of IBR-2M. Possible extensions of the scientific program into the field of nuclear physics have been discussed previously, for example, in [65, 66].

At present, the second-generation IBR-2M reactor is nearing the end of its service life. A natural need has therefore arisen to design a new, higher-power reactor. Despite repeated proposals of scientific solutions to the instability problem, attempts continue to replicate the design of the problematic second-generation reactor. The current challenge is to convince the scientific and technical community of JINR of the lack of prospects for developing a pulsed reactor based on plutonium dioxide using outdated design approaches.

Acknowledgements

The authors are grateful to the Editorial Board of the journal for the invitation to write this article. And we hope that the fundamentals of physics of pulsed periodic reactors presented here will be further developed.

Conflicts of interest

The authors declare no conflicts of interest.

References

- [1] E. P. Shabalin, Pulsed fast neutron reactors. Moscow: Atomizdat, 1976, 206 p. (in Russian).
- [2] I. I. Bondarenko, Yu. Ya. Staviskii, A fast-neutron pulse reactor, *The Soviet Journal of Atomic Energy* 10 (1959) 430–438.
- [3] D. I. Blokhintsev, The birth of the peaceful atom. Moscow: Atomizdat, 1977, 176 p. (in Russian).
- [4] G. E. Blokhin, D. I. Blokhintsev, Yu. A. Blyumkina et al., Pulsed fast-neutron reactor, *The Soviet Journal of Atomic Energy* 10 (1962) 430–445.
- [5] V. D. Ananiev, D. I. Blokhintsev, B. N. Bunin et al., Experience in the operation and development of periodically pulsed reactors in Dubna, fast burst reactors: Proceedings of the Conference USAEC CONF-690102, 1969, P. 173–207; JINR Preprint 13-4395. Dubna, 1969, 35 p.
- [6] I. M. Frank, Scattering of neutrons by nuclei, elementary particles. Moscow: Atomizdat 4 (1972) 806–830 (in Russian).
- [7] V. V. Nitts, Z. G. Papulova, I. Sosnowska, E. Sosnowski, Investigation of structures by neutron diffraction on the pulsed fast reactor IBR, *Fizika Tverdogo Tela* 6 (5) (1964) 1370–1377 (in Russian).
- [8] V. L. Aksenov, A. M. Balagurov, Neutron diffraction on pulsed sources, *Physics-Uspekhi* 59 (3) (2016) 279–303. doi:10.3367/UFNe.0186.201603e.0293.
- [9] V. D. Ananiev, P. S. Antsupov, S. P. Kapitsa et al., A 30 MeV microtron injector for a pulsed fast neutron reactor, *Journal of Nuclear Energy. Part C: Plasma Physics, Accelerators, Thermonuclear Research* 8 (6) (1966) 601–608.
- [10] B. N. Bunin, V. M. Levin, S. K. Nikolaev et al., Startup of the IBR-30 reactor in the pulsed booster mode. JINR Preprint 13-6213. Dubna, 1972, 14 p.
- [11] V. I. Lushchikov, Yu. N. Pokotilovskii, A. V. Strelkov, F. L. Shapiro, Observation of ultracold neutrons, *JETP Letters* 9 (1) (1969) 23–25.
- [12] A. V. Strelkov, Neutron storage, *Physics-Uspekhi* 47 (5) (2004) 511–515. doi:10.1070/PU2004v047n05ABEH001753.
- [13] E. V. Lychagin, D. P. Kozlenko, P. V. Sedyshev, V. N. Shvetsov, Neutron physics at JINR — 60 years of the I. M. Frank Neutron Physics Laboratory, *Physics-Uspekhi* 59 (3) (2016) 254–278. doi:10.3367/UFNe.0186.201603c.0265.
- [14] V. L. Aksenov, Four decades of neutron investigations in Dubna, *Herald of the Russian Academy of Sciences* 71 (3) (2001) 244–249.
- [15] Scientific cooperation of socialist countries in nuclear physics. Ed. by N. N. Bogoliubov. Moscow: Energoatomizdat, 1986, 263 p. (in Russian).
- [16] V. L. Aksenov et al., Proposal for a new type of periodic pulsed reactor with a cold neutron source. JINR Preprint E3-92-110. Dubna: JINR, 1992, 12 p.
- [17] E. P. Shabalin, G. N. Pogodaev, On the optimization of a pulsed fast-neutron reactor. JINR Communication No. 2708. Dubna, 1966, 18 p.
- [18] Summary of SORA project report, pulsed neutrons and their utilization: Proceedings of the Joint Meeting EURATOM–Japan Atomic Energy Society. EUR 4954e. 1973, P. 1–15.
- [19] V. Raievski, The pulsed fast reactor as a source for pulsed neutron experiments, pulsed neutron research: Proceedings of a Symposium. Vol. II. Vienna: IAEA, 1965, P. 533–544.
- [20] J. M. Hendrie, K. C. Hoffmann, H. J. C. Kouts et al., Brookhaven pulsed fast research reactor. Report BNL-13208. Upton, NY: Brookhaven National Laboratory, 1969, 45 p.
- [21] E. P. Shabalin, Power oscillations and stability limit of pulsed reactors, *Soviet Atomic Energy*. 61 (6) (1987) 981–987.
- [22] E. P. Shabalin, Power instability and stochastic dynamics of periodic pulsed reactors, *Nuclear Technology* 99 (3) (1992) 280–288.

- [23] V. D. Ananiev et al., Physical startup of the IBR-2 pulsed research reactor, *Soviet Atomic Energy* 46 (6) (1979) 504–510.
- [24] V. D. Ananiev et al., Power startup of the IBR-2 reactor and the first physics investigations in its beams, *Soviet Atomic Energy* 57 (4) (1984) 731–739.
- [25] V. D. Ananiev, D. I. Blokhintsev, V. S. Smirnov et al., Features of design and optimization of the reactivity modulator for the IBR-2 reactor, *Peaceful Uses of Atomic Energy: Proceedings of the Fourth International Conference*. Vol. 7. Vienna: IAEA, 1972, P. 41–52.
- [26] V. D. Ananiev, D. I. Blokhintsev, Yu. M. Bulkin et al., IBR-2: A periodically pulsed reactor for neutron research, *Instruments and Experimental Techniques* 20 (5) (1977) 1235–1252.
- [27] V. D. Ananiev, V. L. Lomidze, A. D. Rogov, V. S. Smirnov, E. P. Shabalin, Optimization study of the reactivity modulator for the periodically pulsed fast reactor, *Atomkernenergie-Kerntechnik* 43 (4) (1983) 253–259.
- [28] V. L. Lomidze, K. Noack, A. D. Rogov, E. P. Shabalin, Experimental and theoretical research on the promising IBR-2 reactivity modulator, *Soviet Atomic Energy* 67 (5) (1989) 795–802. [doi:10.1007/BF01126129](https://doi.org/10.1007/BF01126129).
- [29] E. P. Shabalin, V. I. Konstantinov, A. D. Rogov, Reactivity modulator. USSR Inventor's Certificate No. 457402. Filed Nov. 26, 1971. Published Jan. 15, 1975.
- [30] D. V. Shirkov, Sixty years of broken symmetries in quantum physics (from the Bogoliubov theory of superfluidity to the Standard Model), *Physics-Uspekhi* 52 (6) (2009) 549–557. [doi:10.3367/UFNe.0179.200906d.0581](https://doi.org/10.3367/UFNe.0179.200906d.0581).
- [31] H. R. Glyde, Deep inelastic neutron scattering and momentum distributions in quantum liquids, *Physica B: Condensed Matter* 194–196 (1994) 505–506. [doi:10.1016/0921-4526\(94\)90582-7](https://doi.org/10.1016/0921-4526(94)90582-7).
- [32] A. I. Babaev, We changed the course of time: Interview, Dubna. Nauka. Sodruchestvo. Progress 49–50 (2009) 6–7 (in Russian).
- [33] V. L. Aksenov, Yu. V. Nikitenko, Neutron standing waves investigations with polarized neutrons, *Physica B: Condensed Matter* 267–268 (1999) 313–319. [doi:10.1016/S0921-4526\(99\)00023-X](https://doi.org/10.1016/S0921-4526(99)00023-X).
- [34] V. L. Aksenov, V. K. Ignatovich, Yu. V. Nikitenko, Neutron standing waves in layered systems, *Crystallography Reports* 51 (5) (2006) 734–753. [doi:10.1134/S1063774506050038](https://doi.org/10.1134/S1063774506050038).
- [35] V. L. Aksenov, V. V. Zhaketov, Yu. V. Nikitenko, Neutron reflectometry with detection of the secondary radiation: Particle–wave method of determining the nanoscale isotope density distributions, *Physics of Particles and Nuclei* 54 (5) (2023) 756–775. [doi:10.1134/S1063779623040044](https://doi.org/10.1134/S1063779623040044).
- [36] D. A. Korneev, V. V. Pasyuk, A. V. Petrenko, E. B. Dokukin, Neutron reflectivity studies on superconducting, magnetic and absorbing thin films at the pulsed reactor IBR-2. In: Zabel H., Robinson I. K. (eds.) *Surface X-Ray and Neutron Scattering*. Berlin: Springer, 1992. P. 213–217. (Springer Proceedings in Physics; Vol. 61).
- [37] D. A. Korneev, V. I. Bodnarchuk, S. P. Yaradaikin, Polarized neutron spectrometer REFLEX-P, Preprint JINR P3-2002-189. Dubna: JINR, 2002. 10 p. (in Russian).
- [38] V. L. Aksenov et al., The polarized neutron spectrometer REMUR at the pulsed reactor IBR-2, JINR Preprint D13-2004-47. Dubna: JINR, 2004. 35 p.
- [39] M. V. Avdeev et al., Neutron time-of-flight reflectometer GRAINS with horizontal sample plane at the IBR-2 reactor: Possibilities and prospects, *Crystallography Reports* 62 (6) (2017) 1002–1008. [doi:10.1134/S1063774517060025](https://doi.org/10.1134/S1063774517060025).
- [40] V. D. Ananiev, A. A. Belyakov, M. V. Bulavin, E. N. Kulagin et al., The world's first pelletized cold neutron moderator at a neutron scattering facility, *Nuclear Instruments and Methods in Physics Research Section B: Beam Interactions with Materials and Atoms* 320 (2014) 70–74. doi.org/10.1016/j.nimb.2013.12.006
- [41] O. G. Buzykin, A. V. Kazakov, E. P. Shabalin, On the theory of pneumotransport of beads in the cold neutron moderator of the IBR-2 reactor, *Physics of Particles and Nuclei Letters* 14 (3) (2017) 520–532. [doi:10.1134/S1547477117030062](https://doi.org/10.1134/S1547477117030062).

- [42] A. K. Popov, Khan Hi Tche, E. P. Shabalin, Analysis of reactivity fluctuations in the IBR-2 reactor, JINR Communication P13-87-808. Dubna, 1987. 8 p. (in Russian).
- [43] A. P. Kuznetsov, S. P. Kuznetsov, Critical dynamics of one-dimensional maps. Part 1. Feigenbaum Scenario, *Izvestiya VUZ. Applied Nonlinear Dynamics* 1 (1) (1993) 15–32 (in Russian). [doi:10.18500/0869-6632-1993-1-1-15-33](https://doi.org/10.18500/0869-6632-1993-1-1-15-33).
- [44] M. M. Podlesnyy, E. P. Shabalin, Ya. A. Vdovin, I. V. Kushnir, A. E. Verkhoglyadov, Bending of fuel assemblies in the IBR-2M reactor and their influence on reactivity, JINR Communication P13-2025-54. Dubna, 2025. 18 p. (in Russian).
- [45] E. P. Shabalin, Influence of fuel pellet jamming on the character of power feedback in a pulsed reactor, JINR Communication P13-2025-13. Dubna, 2025. 12 p. (in Russian).
- [46] A. E. Verkhoglyadov, Motion equation of temperature induced plane transversal vibrations of a rod: Numerical–analytical solution, *Physics of Particles and Nuclei Letters* 20 (4) (2023) 656–660. [doi:10.1134/S1547477123040660](https://doi.org/10.1134/S1547477123040660).
- [47] A. E. Verkhoglyadov, V. N. Verkhoglyadova, E. P. Shabalin, Mathematical model of a periodic pulsed reactor, *Atomic Energy*. 138 (1–2) (2025) 34–40. [doi:10.1007/s10512-025-01220-0](https://doi.org/10.1007/s10512-025-01220-0)
- [48] V. D. Ananiev, N. P. Antsupov, A. V. Vinogradov et al., Startup and investigation of the main characteristics of the IBR-2 reactor with a new heterogeneous reactivity modulator. JINR Communication P13-2004-156. Dubna, 2004. 18 p. (in Russian).
- [49] A. E. Verkhoglyadov, E. P. Shabalin, Model of IBR-2 reactor dynamics based on a two-component power feedback. JINR Communication P13-2025-15. Dubna, 2025. 11 p. (in Russian).
- [50] G. A. Bat', A. S. Kochenov, L. P. Kabanov, Research nuclear reactors. Moscow: Atomizdat, 1972. 272 p. (in Russian).
- [51] V. L. Aksenov, V. D. Ananiev, G. G. Komyshev, A. D. Rogov, E. P. Shabalin, On the limit of neutron fluxes in pulsed sources based on the fission reaction, *Physics of Particles and Nuclei Letters* 14 (5) (2017) 547–554. [doi:10.1134/S1547477117050028](https://doi.org/10.1134/S1547477117050028).
- [52] W. Seifritz, P. Wydler, Criticality of neptunium-237 and its possible utilization in nuclear reactors, *Nuclear Science and Engineering* 72 (2) (1979) 272–276. [doi:10.13182/NSE79-A19473](https://doi.org/10.13182/NSE79-A19473).
- [53] R. Sanchez, D. Loaiza, R. Kimpland et al., Criticality of a ^{237}Np sphere, Proceedings of the International Conference on Nuclear Criticality Safety. Tokai, Japan, 2003. JAERT-Conf 2003-019. P. 201–205.
- [54] K. Miernik, Beta-delayed neutron energy spectrum calculated in the effective density model, *Acta Physica Polonica B* 46 (3) (2015) 717–720. [doi:10.5506/APhysPolB.46.717](https://doi.org/10.5506/APhysPolB.46.717).
- [55] H. H. Saleh, T. A. Parish, W. H. Miller, H. Oigawa, S. Raman, Measurements of the number of neutrons emitted per fission in a fast neutron spectrum for ^{235}U , ^{237}Np , and ^{243}Am , *Nuclear Instruments and Methods in Physics Research Section B: Beam Interactions with Materials and Atoms*. 103 (4) (1995) 393–400. [doi:10.1016/0168-583X\(95\)00658-3](https://doi.org/10.1016/0168-583X(95)00658-3).
- [56] W. S. Charlton, T. A. Parish, S. Raman, N. Shinohara, M. Andoh, Measurements of the neutron capture cross section for ^{237}Np in the energy range from 0.05 eV to 1 keV, Proceedings of the International Conference on Nuclear Data for Science and Technology. Trieste, Italy, (1997) 491–493.
- [57] E. K. Hyde, I. Perlman, G. T. Seaborg, The nuclear properties of the heavy elements. Vol. 1. Systematics of nuclear decay. Englewood Cliffs, NJ: Prentice-Hall, 1964.
- [58] V. N. Konev, Neptunium-237: Properties, structure of alloys and compounds. Preprint No. 11 (68) Moscow: VNIINM, 1981. 45 p. (in Russian).
- [59] S. V. Alekseev, V. A. Zaitsev, Nitride fuel for nuclear power engineering, Moscow: Tekhnosfera, 2013. 240 p. (in Russian).
- [60] Y. Arai et al., Fabrication of nitride fuels for transmutation of minor actinides, *Journal of Nuclear Materials* 320 (1–2) (2003) 18–24. [doi:10.1016/S0022-3115\(03\)00163-6](https://doi.org/10.1016/S0022-3115(03)00163-6).

- [61] K. Minato, M. Takano, H. Otobe, T. Nishi, M. Akabori, Y. Arai, Thermochemical and thermo-physical properties of minor actinide compounds, *Journal of Nuclear Materials* 389 (1) (2009) 23–28. doi:10.1016/j.jnucmat.2009.01.003.
- [62] H. Shibata, T. Tsuru, T. Nishi, M. Hirata, Y. Kaji, Thermodynamic properties of neptunium nitride: A first-principles study, *Journal of Nuclear Science and Technology* 49 (3) (2012) 280–285. doi:10.1080/00223131.2012.660017.
- [63] V. F. Kolesov, *Aperiodic pulsed reactors*, Sarov: RFNC-VNIIEF 1 (2007) 552 ISBN 978-5-9515-0091-5 (in Russian).
- [64] P. P. Dyachenko, G. N. Fokin, Reactor-laser system and a neptunium pulsed reactor, the Scientific and Technical Conference “Neutron-Physics Problems of Nuclear Power Engineering (Neutronika-2016)”, Obninsk, November 23–25, 2016 (in Russian).
- [65] V. L. Aksenov, A report to the Program Advisory Committee for Condensed Matter Physics of JINR, January 19, 2017. JINR Communication E3-2017-12. Dubna: JINR, 2017. 12 p.
- [66] V. L. Aksenov, M. V. Rzyanin, E. P. Shabalin, Research reactors at JINR: Looking into the future, *Physics of Particles and Nuclei* 52 (6) (2021) 1019–1035. doi:10.1134/S1063779621060034.